Universidade de Lisboa

Faculdade de Ciências

(Departamento de Física)

Development of a Rapid Prototyping method for Hard Polymer Microfluidic Systems tested through iterative design of a PCR chamber chip

Miguel Barreiros

Dissertação

Mestrado Integrado em Engenharia Biomédica e Biofísica

Perfil em Engenharia Clínica e Instrumentação Médica

2014

Universidade de Lisboa

Faculdade de Ciências

Departamento de Física

Development of a Rapid Prototyping method for Hard Polymer Microfluidic Systems tested through iterative design of a PCR chamber chip

Miguel Barreiros

Dissertação

Mestrado Integrado em Engenharia Biomédica e Biofísica

Perfil em Engenharia Clínica e Instrumentação Médica

Orientadores: Dr. Hugo Ferreira

Samuel K. Sia, PhD

Abstract

One of the challenges of working with polymer microfluidics is the lack of an established prototyping method which allows for easy translation to industrial production. By combining Hot Embossing and Computer Numerically Controlled Milling a microfluidic rapid prototyping method was established for Polycarbonate and Cyclic Olefin Polymer. This method was then tested and optimized through an iterative design process of a microfluidic Polymerase-Chain Reaction chamber. The fabrication method proved to be suitable for microfluidic prototyping, allowing for rapid design changes and fabrication of good quality copies in a simple and straightforward fashion.

Keywords: Microfluidics, Hot Embossing, Rapid Prototyping, Hard Polymers, Fabrication, PCR

Resumo

Uma das dificuldades em trabalhar com microfluídica em polímeros é a falta da existência de um método de prototipagem que permita uma passagem simples para um ambiente de produção industrial. Neste trabalho foi desenvolvido um método de prototipagem rápida para microfluídica em Policarbonato e Cyclic Olefin Polymer utilizando uma Fresadora de Controlo Numérico Computorizado e Hot Embossing. Este método foi testado e optimizado através de um processo de design iterativo de uma câmara microfluídica de Reacção em Cadeia da Polimerase em Policarbonato. O método desenvolvido provou ser adequado para prototipagem microfluídica, permitindo alterações rápidas ao desenho e fabricação de várias cópias com boa qualidade de cada desenho.

Palavras-chave: Microfluídica, Hot Embossing, Estampagem a Quente, Prototipagem Rápida, Polímeros Duros, Fabricação, PCR

Contents

List of Figures

List of Tables

List of Used Acronyms

CAD	Computer-Aided Drawing
CAM	Computer-Aided Manufacturing
CF-PCR	Continuous Flow Polymerase-Chain Reaction
CNC	Computer Numerical Control
COP	Cyclic Olefin Polymer
DOC	Depth of Cut
HE	Hot Embossing
IM	Injection Molding
IPA	Isopropyl alcohol
MEMS	Microelectromechanical systems
PC	Polycarbonate
PCR	Polymerase-Chain Reaction
PDMS	Polydimethylsiloxane
POC	Point-of-Care
RPM	Rotations per minute
SL	Soft Lithography
SW	SolidWorks
UHSM	Ultra High Speed Machining

1. Motivation

Microfluidics as a research field has seen exponential growth in the last decades. Unfortunately, there have been few truly successful products reaching the market. This gap is mostly due to the difference in fabrication methods between research and production settings. There is a need for a rapid prototyping method that allows for simple translation from a prototyping environment to a cost-efficient industrial fabrication one. For many microfluidic applications the chips need to be durable, disposable and inexpensive. This has been accomplished by fabricating the chips in hard plastic through Injection Molding (IM) as this method is very cost-efficient for large-scale fabrication. IM however does not allow for rapid prototyping as each design change requires extensive optimization.

With that in mind, a rapid prototyping method for hard plastic microfluidics was developed using Hot Embossing (HE). HE allows the fabrication of hard plastic microfluidic structures without extensive optimization and is a good candidate for rapid prototyping when combined with a fast mold fabrication method. Most of the previous work on HE has been done using labor-intensive molds and is not applicable to a rapid prototyping scenario. The choice of mold fabrication method will determine the cost and time necessary to fabricate a chip with a new design. In this work Computer Numerical Controlled (CNC) milling was chosen because it is an extremely versatile technology which has previously been used to mill micro structures in metal substrates.

This method was tested and optimized in the development of a microfluidic Polymerase-Chain Reaction (PCR) chip through iterative design. The development of a PCR chip is a non-trivial challenge and it was necessary that the fabrication method could produce different designs fast and cheaply so as to quickly identify and correct problems along the design process. This allowed testing the suitability of the fabrication method in a research setting.

In the first part of this work a small introduction to microfluidics and microfluidic fabrication is presented, with added emphasis on HE and Mold Fabrication. A brief introduction to PCR miniaturization is presented to better understand the potential of a microfluidic PCR chip and the challenges associated with its development.

In the next section a description of the experimental methods is presented followed by the results obtained using the fabrication method developed to iterate on a PCR chip design. The experimental work began with testing different hot embossing protocols and mold fabrication methods. For the following work, CNC milling was chosen as the mold fabrication method due to the durability of the molds and the versatility of the technique. The PCR chip development began with the adaption of an existing design which was iterated as needed. During the iterative design process the fabrication method was continually optimized to obtain a more robust protocol.

2. Microfluidic Fabrication

This section begins with a small introduction to microfluidics and the history of the field to help understand the state-of-the-art and the influence of the different fabrication methods in the systems developed. The physical characteristics of micro-scale systems are then briefly analyzed to better understand the possibilities and limitations of a microfluidic device.

The most relevant microfluidic fabrication methods are then described in detail and compared in terms of their limitations and applicability to rapid prototyping. Mold fabrication methods are also highlighted as they are critical in a rapid prototyping scenario.

Afterwards, a brief introduction to PCR amplification and the miniaturization of the process are given so that the design goals are well understood.

2.1. Brief History of Microfluidics

Microfluidics as a field began in the 1990's, based on the knowledge acquired developing microelectromechanical systems (MEMS) which themselves were based on knowledge developed on the miniaturization of electronic devices. During the 1970's the miniaturization of electronics produced different silicon technologies such as dry and wet etching or photolithography, which also allowed the machining of miniaturized mechanical devices. These consisted mostly of physical sensors (pressure, acceleration, etc) combined with integrated electronic circuits [1].

MEMS continued to be developed, with several commercial applications reaching the market - inkjet printer cartridges and digital micromirror devices (DMD) for DLP projectors, for example. In the late 1980's several MEMS capable of fluid control were developed – microflow sensors, micropumps, microvalves – and this marked the start of the microfluidics field. After the reviews by Manz et al, in 1990 [2], presenting the biomedical applications of microfluidic systems, the field grew rapidly with intensive research focused in miniaturizing chemical processes. The main goal was to take advantage of the effects of the small-scale in fluid behavior.

With this in mind, through the 1990's many fabrication technologies were developed which eschewed silicon as the substrate for other materials more suitable for prototyping or with other more desirable characteristics such as glass, for bio-applications. The development of Soft Lithography (SL) by the Whitesides group [3], [4] lowered the barrier of entry into the microfluidics world, removing the need for a clean room or wet chemistry and allowing several research groups to experiment with microfluidic processes.

Among the many developments the most promising continued to be biomedical applications, more specifically the lab-on-a-chip or micro total analysis systems (μTAS) devices, which promised the capability of producing a diagnosis from a sample without any human input, much like a computer produces a numerical answer to a calculation. Although impressive proofs-of-concept were created, and despite some notable exceptions [5], there was a general lack of microfluidic systems reaching the market. This happened mostly due to the high cost of converting a proof-of-concept developed in Polydimethylsiloxane (PDMS) using SL to a commercially viable product, something which many companies failed to do. In the 2000's a few successful microfluidic products were produced using injection-molded thermoplastics due to its low cost of production but the conversion of a design developed in PDMS to one in a thermoplastic is non-trivial [6].

Lately there has been an effort to create highly integrated Point-of-Care devices (POC) capable of rapid diagnosis with minimal effort from the user. Since by definition these devices should be disposable, cheap and resistant, thermoplastics are being seen as the ideal substrate for these devices. There is a push for better prototyping techniques which are relevant to IM production as well as continuing active search for other microfluidic platforms capable of reaching the consumer market.

2.2. Micro vs Macro

Although a description of the size and some capabilities of microfluidic systems has been given, it is necessary to note that microfluidic systems are not usually identical smaller scale copies of macro-scale systems. Some of these differences arise from the differences in fabrication methods and materials but most are due to the different effects of physical forces at different scales. These allow for some of the unique capabilities of microfluidic systems and have a major influence in designing new systems.

One of the most critical points in microfluidic systems is the increase in surface area to volume ratio (*S/V*). As volume (V) scales with L^3 and surface area (S) with L^2, *S/V* scales with L^{-1}. This means that for micro-scale systems surface effects are of greater importance than volume effects – gravity and inertial momentum become negligible whereas surface tension becomes of utmost importance for fluid flow, for example. The magnitude of these effects will change depending on exact feature size and design of the system but they are present in most microfluidic systems.

One example of this is that due to the high surface to volume ratio heat transfer is highly efficient at a micro-scale. This allows for rapid heating and cooling of fluids in microfluidic systems, something which has been used extensively in PCR miniaturization, for example.

In order to better understand the characteristics of microfluidic systems, it is useful to go into some detail about the most common practical differences between a macro and micro-scale systems:

Laminar Flow

Fluids are subject to inertial and viscous forces. Inertial forces are related to changes in the fluid momentum whereas viscous forces are related to the shear stress within the fluid, which can dampen the effects of inertial forces. A measure of the different contribution of inertial and viscous forces to the overall fluid movement is the Reynolds number (eq. 1):

$$(1) \qquad Re = \rho V_D \frac{L}{\eta}$$

Where η is fluid viscosity, ρ is fluid density, V_D is drag velocity and L is the characteristic length. It is observable that Re scales with the characteristic length (L) of the system.

The Reynolds number (*Re*) acts as a good predictor of the type of flow present – a lower number (<1200) indicates a laminar flow, whereas a higher number (>2000) indicates a turbulent flow. A laminar flow is characterized by its homogeneous velocity profile with strong interaction between the fluid and the container walls. Mixing of different fluids in a laminar flow happens only due to diffusion (Figure 1: Example of Laminar Flow in a Microfluidic System. Notice the lack of mixing between fluids. Taken from *[66]*.. In a turbulent flow there is little interaction between the walls and the fluid and vortices, eddies and other turbulences easily appear on the fluid flow.

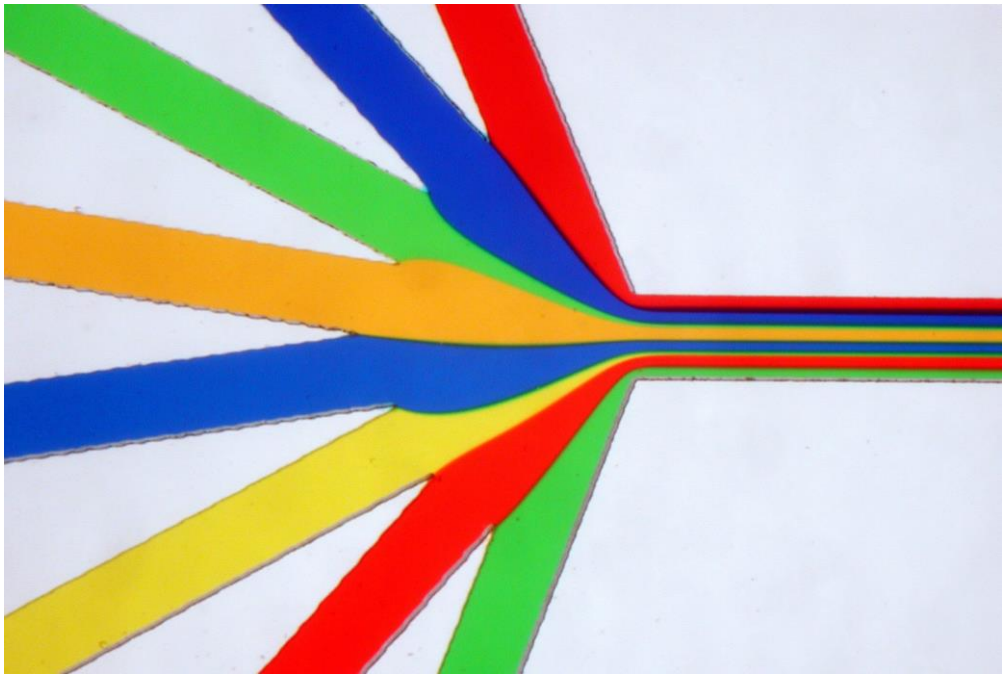

Figure 1: Example of Laminar Flow in a Microfluidic System. Notice the lack of mixing between fluids. Taken from [66].

For flow characterization purposes, microfluidic systems can usually be approximated to a series of continuous channels with different cross-sections. As the distance between channel walls is on the micro-scale, it is possible to obtain laminar flow in conditions (low fluid viscosity, high flow speed) not possible at a macro scale, allowing for precise control of mixing between fluids and overall repeatability of flow patterns. In these conditions when two fluids are present mixing occurs only through diffusion. This has the benefit of allowing for much greater control over fluid mixing but mixing time is usually much longer than at a conventional macro scale, requiring dedicated structures to improve mixing speed. For small sized features (<20 µm) it is also necessary to take into account diffusion transport as at this scale diffusion transport will happen in a short time scale.

Capillary Force

Another consequence of the importance of surface effects at smaller scales is the importance of capillary forces in microfluidic systems. Capillary forces arise from the interaction between a liquid superficial layer and a solid surface and can interfere with the motion of the liquid – depending on the surface properties of the liquid and the solid it might prevent or ease fluid motion. At a micro-scale capillarity is a critical effect that usually has to be explicitly taken into account in the design of microfluidic systems. It can be used as the main mechanism of generating fluid flow or of creating hydrophobic “valves” in the design, for example.

2.3. Fabrication methods

The most relevant polymeric microfluidic fabrications methods will be reviewed to give some context on the characteristics of HE compared to other methods. The fabrication methods reviewed will be Soft Lithography, the *de facto* standard for microfluidic prototyping in the last decade; IM, the method most suited for production-scale fabrication; and HE itself as it is an integral part of the work presented here.

2.3.1. Soft Lithography

The most commonly used method to fabricate microfluidic systems in a research setting is Soft Lithography. Developed and popularized by the Whitesides group [7] it is a polymer-based method which relies on using PDMS casting over a lithography-created mold. A standard protocol usually begins with designing and printing a UV-Mask. A photoresist, usually SU-8, is spin-coated on a silicon wafer to the desired thickness, exposed to the UV light through the mask and developed, forming a hard mold. After cleaning the mold, the prepared PDMS is cast onto it and cured for a few hours. After the curing step, the PDMS is peeled off from the mold and sealed. The sealing step is usually performed by exposing the PDMS chip to oxygen plasma and attaching to a glass slide. This forms a tight seal between the glass and the PDMS walls.

Before moving on to discussing other microfabrication methods it is important to give a detailed explanation of the major components in SL - the photoresist, namely SU-8; and the substrate, PDMS and comment on the major characteristics of SL.

Photoresists are materials, usually polymers, which are sensitive to light and solidify (negative photoresist) or dissolve (positive photoresist) when exposed to specific light wavelengths. SU-8 is a negative photoresist based on EPON SU-8 epoxy resin for the near-UV wavelengths from 365 nm to 436 nm. At these wavelengths SU-8 has very low optical absorption, which makes photolithography of thick films with high aspect ratios possible. This resist was developed by IBM and was later adapted for MEMS applications during the 1990's [8], [9]. Structure height is usually up to 100 µm per layer with an aspect ratio up to 10. Creating an SU-8 mold is considered to be relatively simple but it does involve some steps (see Figure 2):

Spin Coating – The photoresist is spin-coated on a silicon wafer at a specific speed in order to create a smooth, even layer. Silicon is used due to the strong SU-8 adhesion. The film thickness defines the feature height and is defined by the photoresist viscosity.

Soft Bake – The solvent is evaporated by heating up to 95ºC for 10-45 minutes.

Exposure – The photoresist is exposed to near-UV wavelength light through a mask. This is usually done with a mercury lamp and the mask should be as close as possible to the SU-8 without touching. In order to obtain the best resolution possible it is necessary to use specialized alignment equipment.

Post-Exposure Bake – The exposed sections of the photoresist are cross-linked by heating it up to around 95ºC for 5-10mins.

Developing – A developer is used to remove the non-exposed photoresist. This step usually takes 15-20mins.

ADAPTED FROM [1], [7]

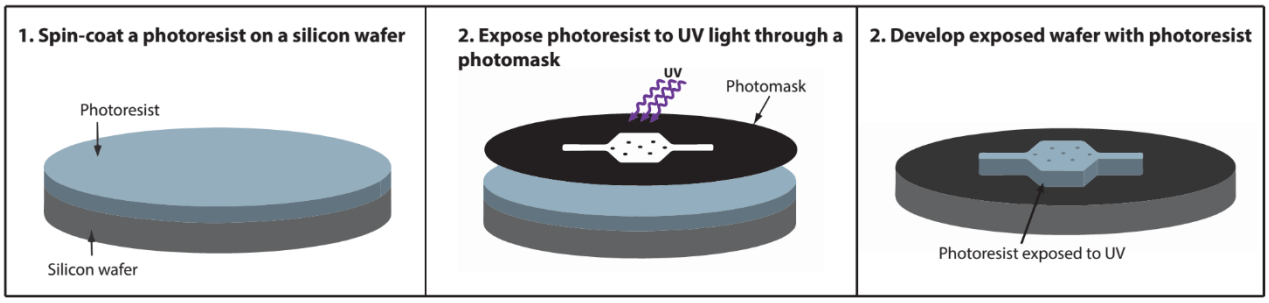

Figure 2: Diagram of the SL master fabrication steps. Adapted from [61]

Although many elastomeric materials can be used for Soft Photolithography, PDMS is by far the most common, mostly due to it being affordable, very simple to use and having some desirable physical properties. Due to its viscoelastic properties it is also present in different commercial products such as shampoos and Silly Putty. Both the prepolymers and the curing agent are easily available and the curing process is robust; it has low toxicity; it is optically transparent and mechanically durable; and its surface energy can be temporarily modified with a plasma treatment.

Its main disadvantage in SL is related to its elastic nature, which allows for structure deformation and limits the designs possible (aspect ratios between 0.2 and 2). PDMS can also swell in the presence of some organic solvents and is relatively permeable to gases although this might be useful in some scenarios (e.g. cell culture)[10] .

In SL, obtaining a PDMS chip from a mold usually involves a few simple steps:

Mixing – the base and the curing agent are mixed with a 10:1 ratio. This ratio can be changed depending on the desired properties (higher ratio produces a harder cured polymer).

Casting – The mixture is poured onto the mold and desiccated in a vacuum chamber for 30-45min.

C*uring* – The polymer is cured on the mold at 60ºC to 80ºC for 1-4 hours.

Sealing – The PDMS is peeled off and exposed to oxygen plasma. The featured side is brought into contact with the sealing material (glass, silica, or oxygen-activated PDMS) and forms a watertight seal.

ADAPTED FROM [1], [7]

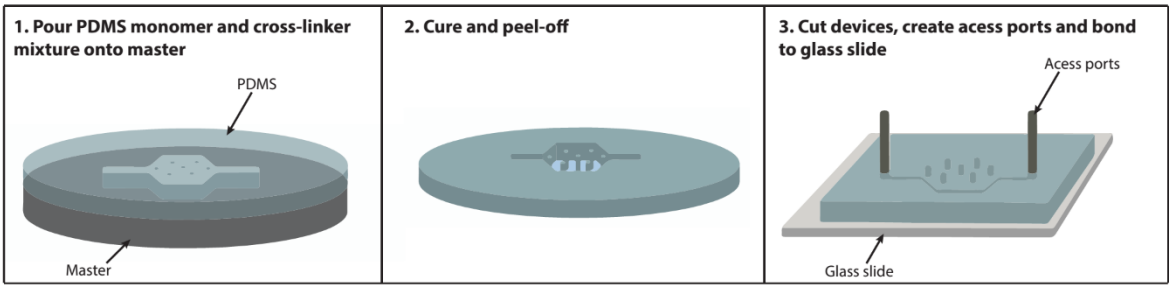

Figure 3: Diagram of the SL PDMS casting steps. Adapted from [61]

SL was adopted as the microfluidic fabrication technique of choice in many research laboratories during the 2000's because it allows the fabrication of complex microfluidic structures and devices in a relatively simple way with a robust method, which make it practical for prototyping different microfluidic designs, especially when coupled with the in-house printing of masks. It is also possible to exploit some of the elastic properties of PDMS to build complex structures such as valves [7] and 3D channels [11].

Soft Lithography's main drawback is the difficulty in adapting both the fabrication process and the designs to a mass-fabrication situation in a cost-efficient way. As has been reviewed above, fabricating a PDMS chip through SL is a multi-step process and the final chips do not achieve the physical stability required for long-term use. It also quite challenging to adapt a chip prototyped in PDMS to other substrates for which industrial production has been developed - mainly injection-molded thermoplastics. These drawbacks have held back the transition of many microfluidic systems from a research setting to real-world applications.

2.3.2. Micro Injection molding

Micro IM is a polymer fabrication process which involves melting a thermoplastic in granule form into a plasticization unit, and injecting it into a microstructured mold (Figure 4). The material is subjected to a holding pressure and after some time it is cooled below the polymer's glass transition temperature and the part is demolded. A typical cycle lasts between few seconds to few minutes [12]–[14].

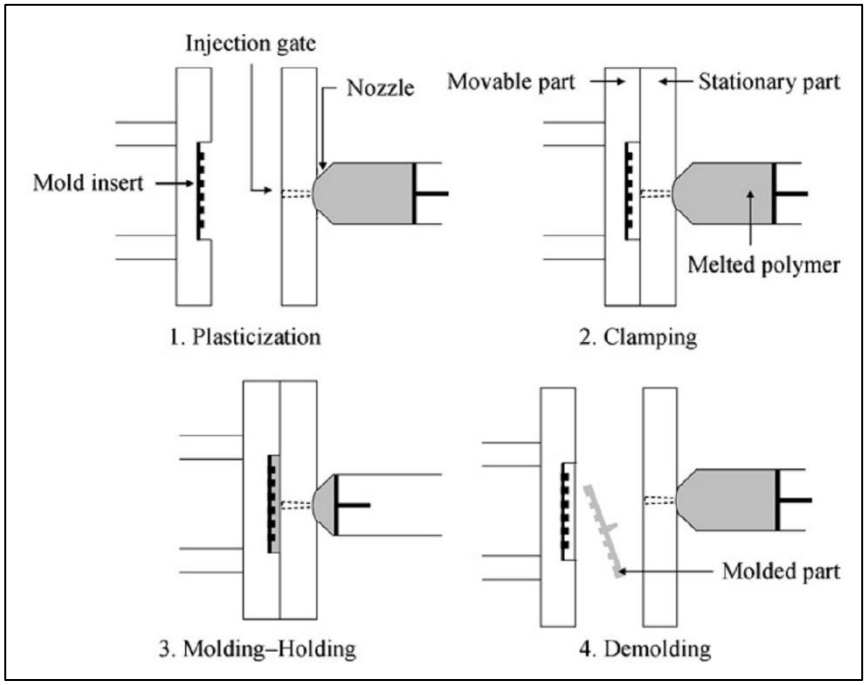

Figure 4: Diagram of an Injection Molding cycle [13].

Micro IM is well suited for the mass production of polymer microfluidic chips due to its short production cycle and associated low production cost per piece. It also allows for the production of relatively complex designs without added fabrication costs. Additionally, conventional IM has been used for the production of many different plastic parts, with different compositions and quality requirements and the knowledge acquired can be used when using Micro IM, automating the production process or using different polymers, for example.

Conventional IM was first developed at the end of the 19th century with major developments during the 20th century allowing for the production of progressively higher quality pieces. Micro IM was first developed in the 1980's using adapted conventional IM machines [12]. The main problems with this approach were the inaccuracy of the hydraulic controls, the waste of material, and the degradation of the material during plasticization which limited the quality of the

final pieces. These were partially solved by using electrical controls, smaller injection screw and barrel and separating the plasticization and the injection (using a hot cylinder and a plunger instead of a screw and a barrel).

Micro IM continued to be developed, with some commercial machines appearing in the last decades [13]. These are capable of fabricating pieces from 0.08 to 8 cm^3 with feature size ranging from sub-micron to tens of microns, depending on the machine. This was achieved through many distinct developments, namely the higher control of different process parameters (volume, pressures, etc), the improvement in the transition from injection pressure to holding pressure, but also through protocol optimization.

It was discovered that a critical parameter in the Micro IM process is the mold temperature during injection. By raising the mold temperature near the T_g of the substrate and cooling it afterwards (before ejection) it is possible to obtain micro-features with higher aspect ratio. This process is called Variotherm in opposition to conventional IM where mold temperature is kept roughly constant. Although necessary for the successful fabrication of small, higher aspect ratio features, it does have some drawbacks. The heating and cooling steps greatly extend the cycle time; and if the cooling is too fast it will introduce stress onto the piece, creating imperfections.

Due to the large number of parameters in a Micro IM process, the dependency of these on different factors (mold material, feature size, total volume, etc), and their major influence in the quality of the fabricated pieces, it is usually necessary and recommended [12], [15] to design and run an optimization experiment whenever an element is changed, such as the substrate material or the mold design. This is the main reason why prototyping a microfluidic design using IM is not an efficient process, as each design change might take one to two weeks of optimization to translate into a quality chip. This problem is compounded by the fact that a lot of the research in Micro IM was developed for commercial reasons and is proprietary knowledge, making it harder for research laboratories acquire the knowledge necessary to efficiently use Micro IM.

It is interesting to note that after parameter optimization feature quality will depend on the mold fabrication method and quality, as in a HE process. As a general rule, mold designs should also be limited to 2.5D features with no undercuts, again similarly to HE.

2.3.3. Hot embossing

Micro HE is a cost-effective replication technology, capable of transferring microstructured patterns from a master mold onto a polymeric substrate. Although some work was done in micro-patterning using hot-embossing before (vinyl LP fabrication), it was during the 1990's that most of micro hot embossing technology development was focused on MEMS production. The technique used was LIGA (**Li**thographie, **G**alvanoformung, **A**bformung) which was capable of producing complex polymeric micro structures with high aspect ratios, something not possible with other fabrication processes at the time.

Thermoplastics consist of unlinked or weakly linked chain-like molecules that at a temperature above the glass transition temperature (T_g) and below the melting temperature (T_m) become plastic and can be molded into specific shapes, which will cure after cooling to temperatures below Tg [16]. Micro HE is a method of exploiting this property to create micro-patterns from a pre-built mold. As the polymer doesn't undergo a phase change during hot embossing, the finished piece presents little residual stress. The reduced temperature variation (compared to IM) also reduces the piece shrinkage during cooling [17].

Developed in the 1990's at Forschungszentrum in Karlsruhe, Germany, LIGA is a stepwise microstructuring process followed by a HE step originally developed using X-ray lithography [18] but which has since been adapted to use electron beam lithography, UV lithography and other similar technologies [1]. It consists of four basic steps: (1) a contact lithography step, traditionally x-ray lithography if high aspect ratio is necessary, (2) an electroplating step to create a metal layer (usually nickel) on top of the patterned substrate, (3) the subsequent stripping of the substrate, with the metal layer (or "shim") acting as the mold, and (4) the hot embossing step. Nowadays UV-LIGA is more common than X-ray LIGA due to its lower cost as it does not require a synchrotron, even though it is not capable of producing features with such a high aspect ratio. The main drawback of using LIGA to fabricate hot embossed microfluidic chips is the lengthy and sensitive electroplating step, which can take up to 2 weeks for each mold, making truly rapid prototyping impractical. The embossing step is usually performed with the use of a highly specialized machine which creates vacuum conditions and is capable of precisely defining temperature and pressure. The demolding process used has the drawback of leaving embossed chips with a relatively rough surface on the unfeatured side. Due to its costly and lengthy process, LIGA is now only used in applications where high aspect ratio and small dimensional tolerances are necessary.

A typical hot embossing process is composed of four major steps (Figure 5 and Figure 6). The process starts with (1) heating of a thin polymer substrate and the mold to molding temperature, followed by (2) an isothermal molding by embossing (velocity- and force-controlled), (3) the cooling of the molded part to demolding temperature, maintaining constant pressure, and (4) demolding of the components (mold and substrate) [19], [20].

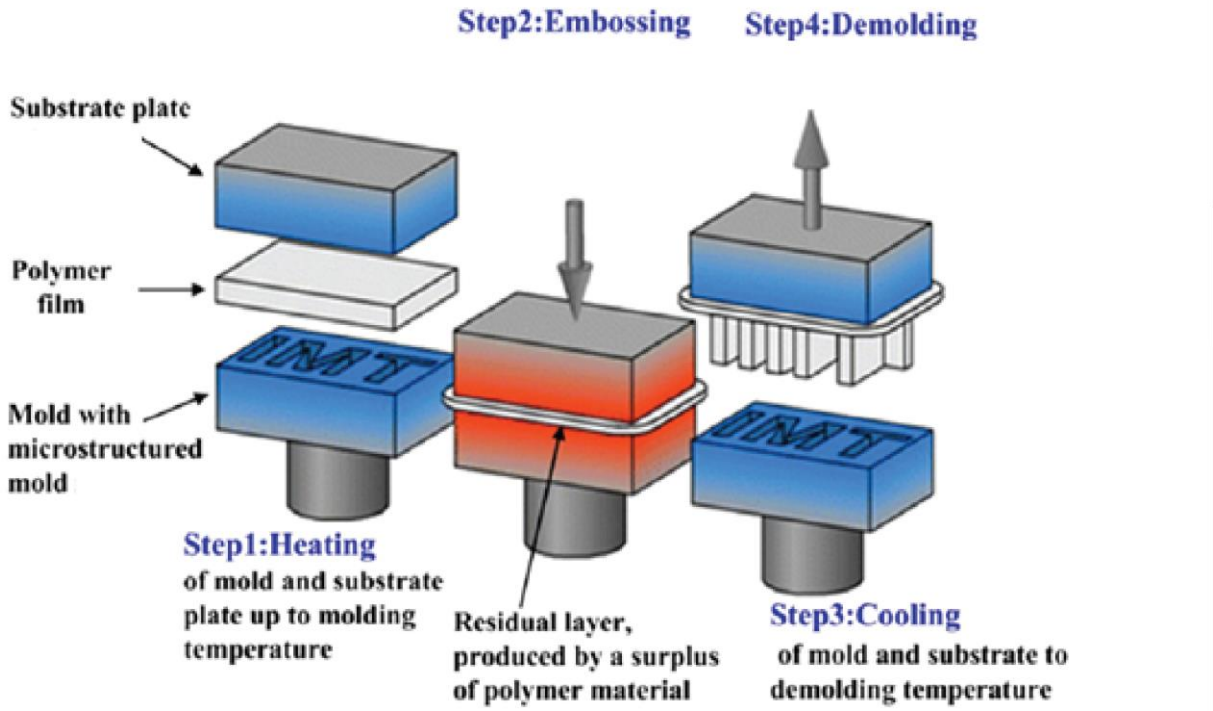

Figure 5 Diagram of a Hot Embossing cycle. Adapted from Lai et al (2013).

On the heating step, temperature control is obviously extremely important and should be accurate within 1ºC of the target temperature. The exact embossing temperature (T_e) will depend on the molded features (high aspect ratio-> higher temperature) and the material used but will usually be around 10-30ºC above the glass transition temperature (T_g). The mold and the substrate should be in contact during heating to make sure they are both at T_e during embossing.

On the embossing step, the pressure increases and the substrate flows radially and into the mold features [20]. The mechanisms for increasing the pressure can range from manually controlled parallel platens pushing the substrate [21] and the mold together to an automated gas-pressure-assisted system to guarantee pressure homogeneity [22]. The pressure is increased slowly to prevent stress on the piece and maintained constant until demolding. By definition only the featured mold area is counted towards the pressure calculation. The residual layer will be thinner for longer

embossing times (t_e) but it will always be present. This step usually takes 10-30mins depending on the complexity of the design and the desired residual layer thickness.

The setup is then cooled actively or passively until the demolding temperature (T_d). T_d depends on the feature design and demolding method and is usually 10-20ºC below T_g. The demolding is the most critical step of the hot embossing process [20], [23] as small changes in T_d can cause a large variation in the force required to demold the piece, influencing the feature quality. If T_d is too high, there will be reflow of the plastic outside of the mold and the features less well defined. If it is too low there will be strong adhesion forces between the feature walls and the mold which will deform the piece upon demolding.

It is now possible to understand that a HE protocol can be nearly completely defined with few simple process parameters: embossing temperature, embossing pressure, embossing velocity, embossing time and demolding temperature. This makes HE a robust process, capable of producing copies with little variability in feature quality [20], [24]. It also allows for easy description of protocols, requiring only the description of the setup and the parameters used (Figure 6).

The main drawbacks of using HE for microfluidic fabrication are related to the difficulty of adapting the process to large-scale fabrication in a cost-efficient way without losing the rapid-prototyping capability. Efficiently fabricating multiple-copies molds, demolding large-area pieces and long cycles are some of problems which have yet to be solved [23], [25].

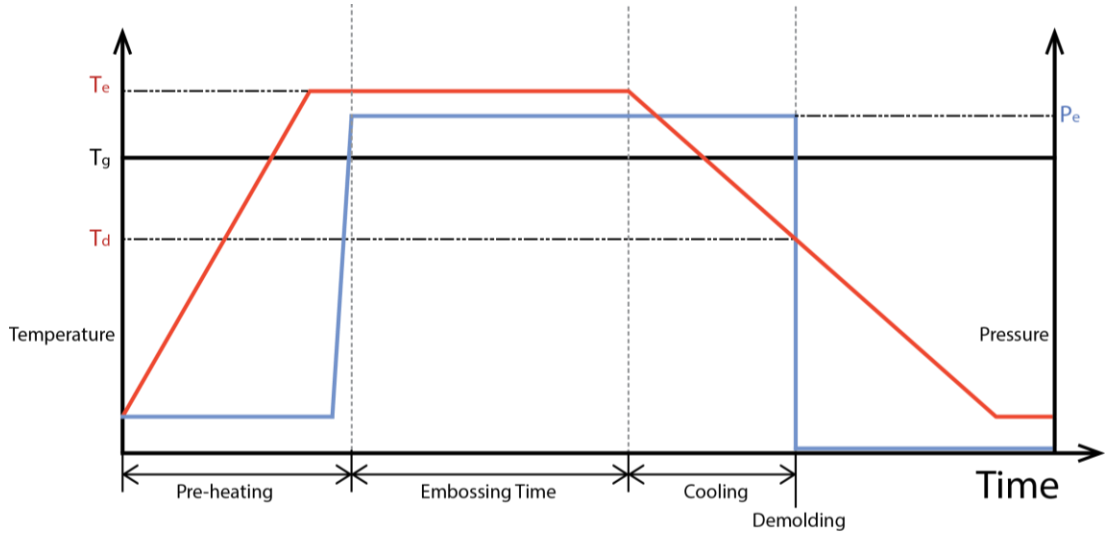

Figure 6: Pressure and Temperature diagram of a Hot Embossing cycle. Ideally a hot embossing protocol can be fully described by an identical diagram. The temperature is in red and the pressure in blue.

Having described the three major polymer microfluidic fabrication methods, it is useful to review their main capabilities and constraints (see Table 1).

IM is a mature technology which has been adapted to successfully produce many different microfluidic designs. Its main advantage is the extremely low cost of making large number of copies of the same design. Each design requires extensive process parameter optimization, making it unsuitable for rapid prototyping.

SL is an extensively used microfluidic fabrication technique which allows for the rapid fabrication of complex designs in elastomeric polymers. Its main disadvantage is the difficulty in transferring a design prototyped in PDMS to a mass-produced (Injection Molded) design in thermoplastic.

HE is a simple, robust fabrication technology capable of producing high quality microfluidic polymer chips. Its main advantage is the capability of producing thermoplastic microfluidic chips with little optimization necessary provided there is a suitable mold. It is straightforward to mass-produce designs prototyped with HE. Its main disadvantage is being unsuitable for large scale production, as it is non-trivial to emboss multiple copies of one design at once and each fabrication cycle takes several minutes, a long time when compared to seconds in IM.

Fabrication Method	**Advantages**	**Disadvantages**
Soft Lithography	Cost-effective, able to fabricate 3D geometries, high resolution	Pattern deformation, vulnerable to defect
Injection Molding	Easy to fabricate complex geometry, fine features, and 3D geometries, low cycle time, mass production, highly automated	Restricted to thermoplastics, high cost mold, difficult to form large undercut geometries
Hot Embossing	Cost-effective, precise, and rapid replication of microstructures with low structural stress	Restricted to thermoplastics, difficult to fabricate complex 3D structures

Table 1: Summary of the various fabrication methods. Adapted from [26].

2.4. Mold Fabrication

Provided the HE setup and protocol are adequate, the quality of hot embossed features depends mostly on the quality of the mold [27]–[29]. It is then of upmost importance to carefully evaluate the mold fabrication process when considering HE for microfluidic fabrication. Different methods will produce molds with different materials and physical properties. HE molds should be thermally resistant up to the embossing temperatures, thermally conductive, rigid and structurally resistant to several embossing cycles. In a rapid-prototyping scenario molds should also be quick and simple to fabricate at a low cost, allowing for multiple design changes.

The most common mold fabrication methods for microfluidic systems are photolithography-based methods (e.g.: SU-8 on silicon wafers, secondary polymeric molds and electroplated molds) and direct-structuring methods (e.g.: micro-milling, micro electric discharge machining, laser structuring). All of these are suitable for different applications outside mold fabrication as well, but are widely used to create HE molds because they are capable of creating permanent surface patterns on the nanometer and micron scale. It is interesting to note that although many microfluidic devices have sub-micron features, most Lab-on-a-chip systems smallest features are over 50 μm [4].

As was mentioned before, Electroplating has been used as a mold fabrication method for hot embossing, usually in a LIGA process [30]. Electroplating is a technique used to coat a metal piece with a thin film of other metal by applying a current between the piece and the source metal. The piece acts as the cathode and the source as the anode with both being immersed in a plating bath whose composition facilitates the electrodeposition reaction. Ideally, the metal coating adheres permanently to the piece.

Although the distinction is sometimes not mentioned in literature, most “electroplated” molds are in fact fabricated through electroforming and not electroplating. Both techniques exploit the electrodeposition phenomenon but whereas electroplating is directed at creating a metal coating on a piece, electroforming is directed at creating a metal piece from a non-metallic master. In electroforming a master form is made conductive through the application of a thin coating and the electrodeposition process is performed identically to an electroplating protocol but it is ran for much longer periods of time so that it forms a thicker layer (up to 1 mm) [31]. The master is then removed and the created metal piece is used as the HE mold, for example. HE molds are usually

made from Nickel due to its rigidity, good thermal properties and ease of use in electrodeposition [32].

Both of this techniques are slow processes with electroforming protocols usually lasting for 1-2 weeks to obtain HE molds with the thickness and quality required [33]. In addition to that, electrodeposition usually requires extensive knowledge and parameter optimization (current applied over time, bath composition) to obtain good results [34]. Its main advantage is the capability of creating metal molds with good surface quality and small feature size (< 1 µm).

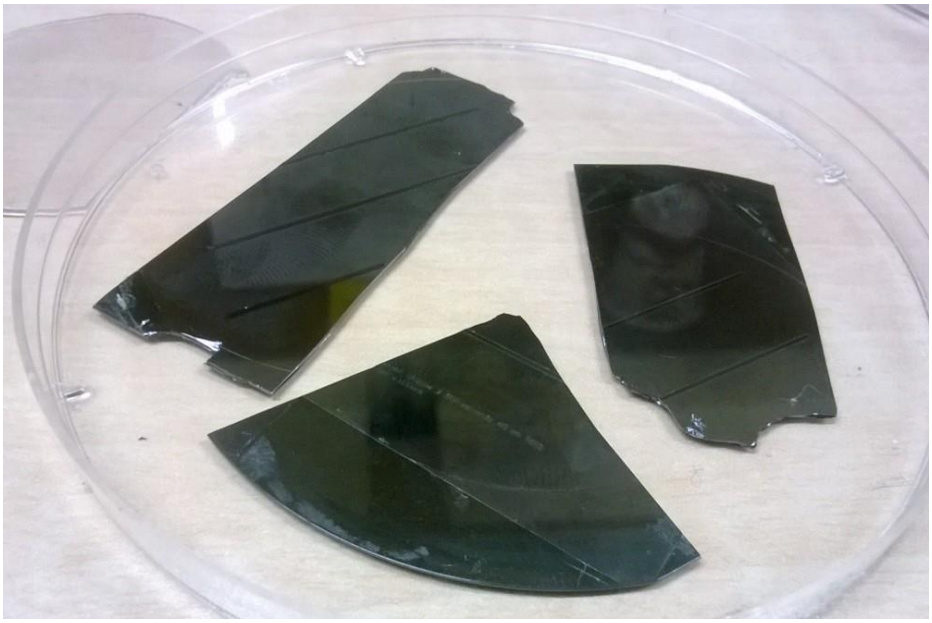

Figure 7: Broken Si wafer with SU-8 features. This is a common occurrence when demolding photolithography molds.

Depending on the goals of the design, using conventional SU-8 photoresist on silicon wafers might be possible [35]. These can allow the use of well-established, versatile lithography methods while being adequate for rapid-prototyping. These usually produce molds less durable than other methods [25]. Common problems with using SU-8 masters are mainly the difficulty in demolding combined with the brittleness of the silicon wafers which usually result in the breaking of the mold after some HE cycles (see Figure 7) [27], [29], [36]. An antistick thin layer might be deposited on the mold to prevent friction and ease demolding [37] but this introduces an extra step into the fabrication. There have also been reports of deformation due to the thermal stress on the SU-8 features after several repetitions [29]. If the goal is to prototype a new chip design, then mold deformation might not be as important as the number of fabricated units with each design is low. Mold breakage might be a problem, depending on the demolding process and the number of copies

required. Photoresist molds usually present very smooth walls and surface finish but are limited to around 100 µm thick features.

Other fabrication methods used in the literature were the casting of secondary molds from SU-8 primary molds in order to overcome the structurally deficiencies of silicon wafers while retaining the advantages of photolithography. Epoxy resin, thermoplastics with high T_g and PDMS [36], [38] have all been used. Overall there were improvements over using SU-8 molds but also some additional problems with this approach, mainly the poor dimensional stability of PDMS and the low embossing temperatures possible with epoxy or thermoplastics. Besides this, all the restrictions of using photolithography are still present with the added step of fabricating a secondary mold.

Another interesting approach is performing SU-8 photolithography on a copper substrate instead of a silicon wafer [37]. This allows for a much stronger mold with better thermal properties while retaining the benefits of using photolithography. Besides the normal photolithography restrictions there is also the added issue of properly polishing and cleaning the copper substrate to obtain good adhesion between the photoresist and the copper wafer.

CNC Milling

Of all the direct structuring methods Computer Numerical Controlled (CNC) milling one of the simplest ones. Milling is the removal of material from a stock piece using rotary cutters (see Figure 8) to form a finished piece. The stock piece can be made of any material able to withstand the milling process, such as wood, metals or polymers. In CNC Milling the tool is controlled by a computer, usually through previously written routines or programs using a numerical control language, G-code.

a)

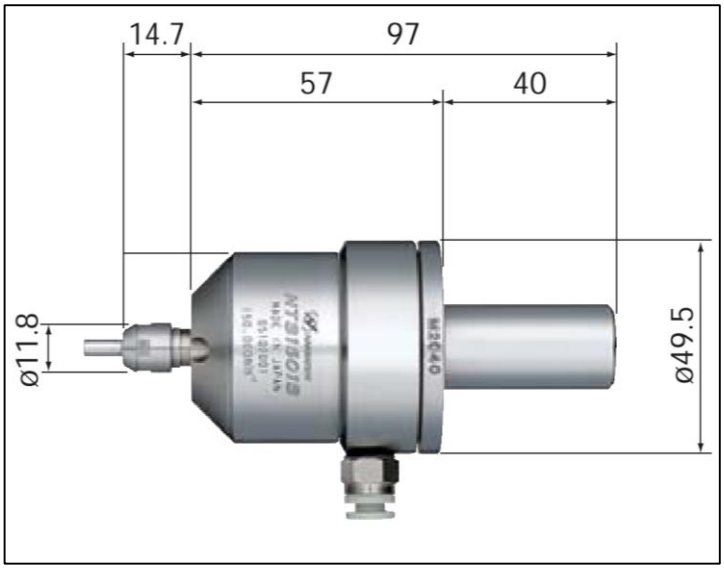

b)

c)

Figure 8: CNC Milling apparatus. a) Conventional Bridgeport CNC Mill; b)High Speed Spindle from NSK. Measures in mm; c) Miniature Endmill cutter. This tool has a 3.175mm shank with 1.5875mm cut diameter. Adapted from [62]

In a normal milling process a rotating cutter moves into the stock piece (this can be achieved by moving the piece, the tool or both) removing small amounts of material with each rotation. The speed at which the tool moves into the piece is called Feedrate (in inches/min or mm/min) and the rotation speed is usually shorthanded to Speed (in RPM) [39]. The depth at which the tool cuts into the material is called depth of cut (DOC).These parameters can be changed and need to be optimized depending on the size of the mill, the material of the piece, the surface finish required and the desired material removal rate. After the definition of these parameters it is necessary to specify the toolpaths necessary to obtain the final piece shape. This can be done “manually” by programming G-code but it is usually done with the help of a Computer Assisted Machining (CAM) program.

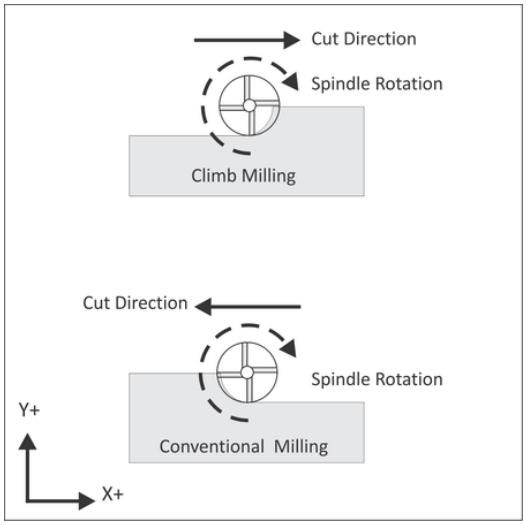

Figure 9: Different milling types. Climb milling is usually chosen for micro-milling but Conventional Milling is used for micro-milling as it minimizes mill deflections perpendicular to the direction of cut.

Micro-milling is the application of CNC Milling to small-sized structures, although the distinction between macro and micro scale milling isn't well defined. Micro-milling, also called micro-machining, has been used to fabricate microfluidic molds with features under 100 µm. The size limiting factors in micro-milling are the size of the tools and the relatively high roughness present in small features. It is extremely well suited for mold fabrication as it allows for arbitrary design changes (including thick features), has few process parameters, and is capable of quickly producing metal molds.

Although the overall principle is identical, there are some differences between normal milling and micro milling. The critical part of milling is maintaining a high angular velocity, to allow the tool to cut into the piece. As the tools become smaller (see Figure 10) this requires having faster rotational speeds with high speed machining (HSM) starting at 10 000 RPM and ultra-high-speed machining (UHSM) at 100 000 RPM. This is a problem in reusing existing CNC mills meant for macro-scale milling as they are usually only capable of speeds up to 10 000 RPM. There are HS and UHS spindles which allow adapting machines for higher speeds but it does represent an additional cost. Other common issue is that CNC mills built for macro-milling usually have a minimum step size (the minimum distance the tool can be moved in any direction) of 1-3 µm which prevents the definition of micron-sized toolpath features. Due to the small size of the tools extra care must be taken to account for the lower rigidity of the tools. As tool breakage is more common than in macro-milling and smaller tools cost more than larger ones, the running costs of micro-milling will also be higher.

Comparing to other mold fabrication techniques, its main disadvantages are the relatively high surface roughness and minimum milling size limitations. The surface roughness can be reduced by optimizing the process parameters or by polishing the mold [40] although it will always be present. Its main advantages are the fast fabrication time, being able to produce metal molds and the low cost per mold.

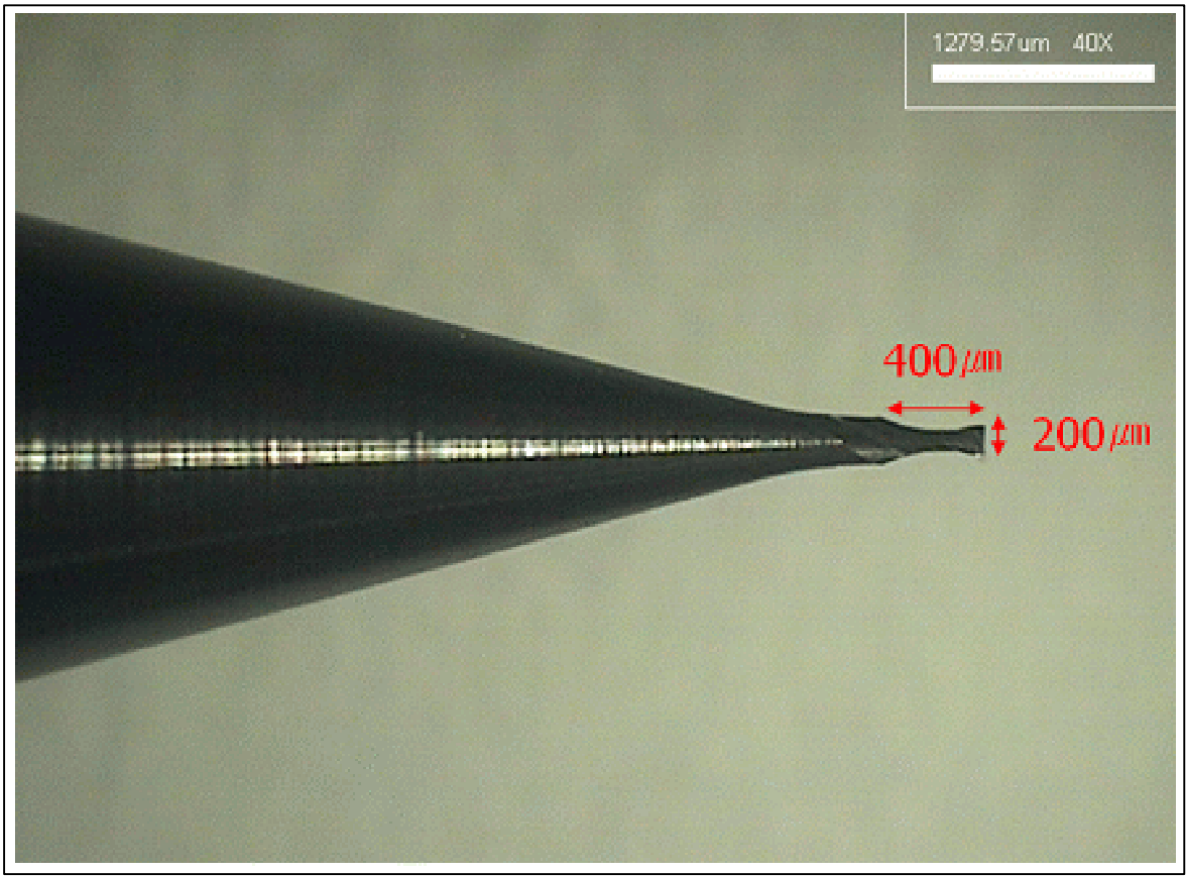

Figure 10: Microphotograph of a micro end-mill with 200 µm diameter. Notice the large size ratio between the shank and the cutting edge diameters. Adapted from [63]

3. PCR

Introduced into the scientific community during the 1980's, PCR is a technique that allows for exponential amplification of DNA without the need to clone into vectors [41]. PCR has become an essential part of biological and biomedical research as well as medical diagnosis. It allows the detection and diagnosis of infectious diseases; genetic analysis of various kinds; forensic analysis, among other uses. PCR-based diagnosis methods allow the detection of pathogens with high sensitivity and sensibility [16], [42].

PCR relies on thermal cycling - heating and cooling the DNA sample to specific temperatures - in the presence of primers, DNA polymerase and *Deoxynucleoside triphosphates (dNTPs)*. Primers are small strands of nucleic acids which are complementary to specific target regions of the DNA strands.

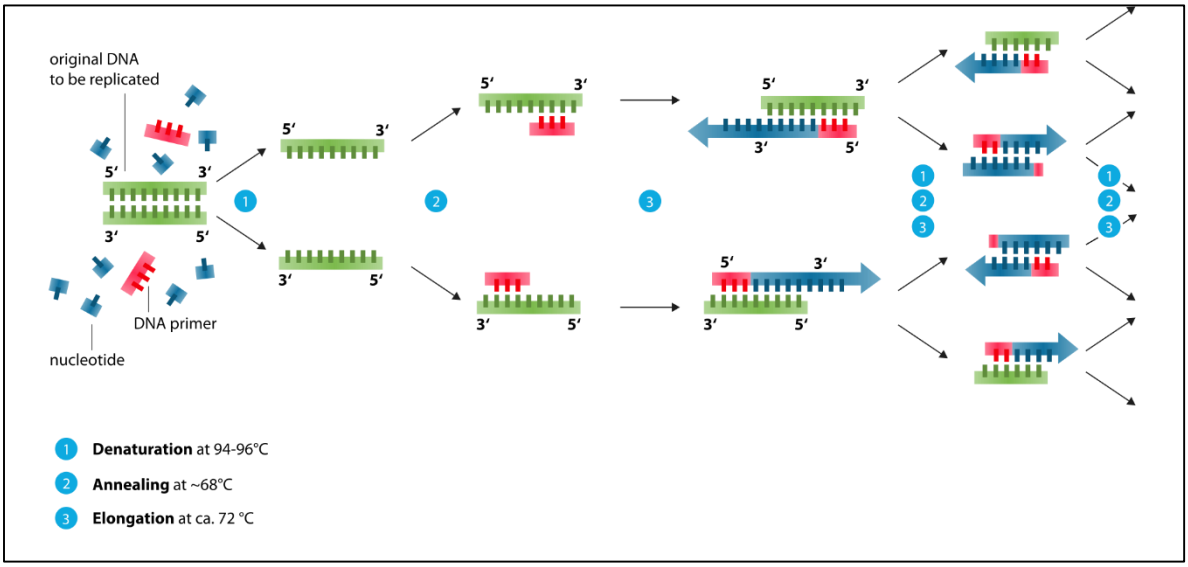

Figure 11: Diagram of a 3-step PCR thermocycling protocol. Adapted from [64]

The conventional PCR protocol consists of 20-35 thermal cycles with each cycle having 3 target temperatures (see Figure 11). There is usually an initialization step at 94-96 ºC before the thermocycling. During the heating (Denaturation) step (94-98 ºC), DNA melting occurs and DNA strands are separated, forming single-stranded DNA molecules. The temperature is then lowered (Annealing step) to 50-65 ºC depending on the primers used. During this step primers attach to single stranded DNA. Temperature is raised again for the elongation step, with the exact

temperature depending on the DNA polymerase used. The DNA polymerase (more commonly Taq polymerase) then synthesizes a complementary DNA strand, initiating the process on the attached primers and using the dNTPs present. This cycle is repeated multiple times, duplicating the target DNA sequence with each cycle and allowing for an exponential amplification.

Over the years, many PCR protocol variants were developed, allowing for multiple primers, different polymerases and faster thermocycling protocols.

3.1. Miniaturization of PCR

"Miniaturization of PCR provides many advantages, such as decreased cost of fabrication and operation, decreased reaction time for DNA amplification, reduced cross talk of the PCR reaction, and ability to perform large numbers of parallel amplification analyses on a single PCR microfluidic chip." [43]

The first PCR microdevices developed were focused on improving the reaction/amplification speed and were fabricated in silicon. Silicon has a high thermal conductivity and allows for very fast temperature ramp times, resulting in very short on-chip protocols [44]. It is also possible to integrate heaters and sensors directly into the chip. Despite these advantages, silicon presents some critical flaws as a PCR-chamber substrate as bare silicon has an inhibitory effect on the PCR reaction and fabricating a functional device required a highly complex protocol and design, and there is a lack of available rapid prototyping techniques. As an alternative, glass was used as a substrate for PCR-chambers in Lab-on-a-chip devices, as it presents well-defined surface chemistry and is optically transparent.

Recently, various polymers have started to become the substrate of choice for PCR-based devices [45], as the focus shifted from reaction speed to integration in Point-of-Care devices. In this case the goal is not just to obtain a faster reaction time but also to obtain PCR amplification using small reagent volumes with little user input in a cheap and disposable chip.

Point-of-care testing is defined as near-patient testing in a hospital, doctor's office, clinic, or home [46] and can have an important impact in low-resource settings where there is a lack of centralized laboratories or when timing is critical, in emergency triage for example [43]. There is also an opportunity in providing rapid, low-cost tests for home or clinic use [47].

Due to the need for POC to be disposable and low-cost, thermoplastic polymers have emerged as the substrate of choice for these devices. As was mentioned above, IM allows for the mass-production of microfluidic chips at a low cost per device.

There have been some academic [48]–[51] and some commercial solutions [52] but there has yet to appear an example of a truly simple to use integrated platform. So far all FDA-cleared PCR test kits to-date are still categorized as high or moderate complexity [53], meaning they are still required to be used by a trained professional. This has happened due to the difficulty in integrating many different functions, namely sample preparation, amplification and detection, necessary for a PCR-based diagnostic device while retaining a simple, low-cost design. POC device development requires the focus on the final application to be present along the development process, so that end-use restrictions are accounted for at every step of the process.

In terms of PCR miniaturization, it is useful to note that most of the approaches can be classified into either single-chamber PCR or Continuous Flow PCR (CF-PCR) (see Figure 12). Single-chamber designs were the first ones to be developed and are characterized by their smaller minimum sample volume and simpler system configuration. A chamber is filled with PCR reagent mixture and some form of temperature control heats the contents, identical in function to a conventional thermocycler.

In a CF-PCR design the PCR mixture is transported over different zones of the chip, with each zone at different pre-fixed temperatures in order to emulate thermocycling. CF-PCR designs are usually characterized by simpler thermal control mechanisms and the need to have precise flow control.

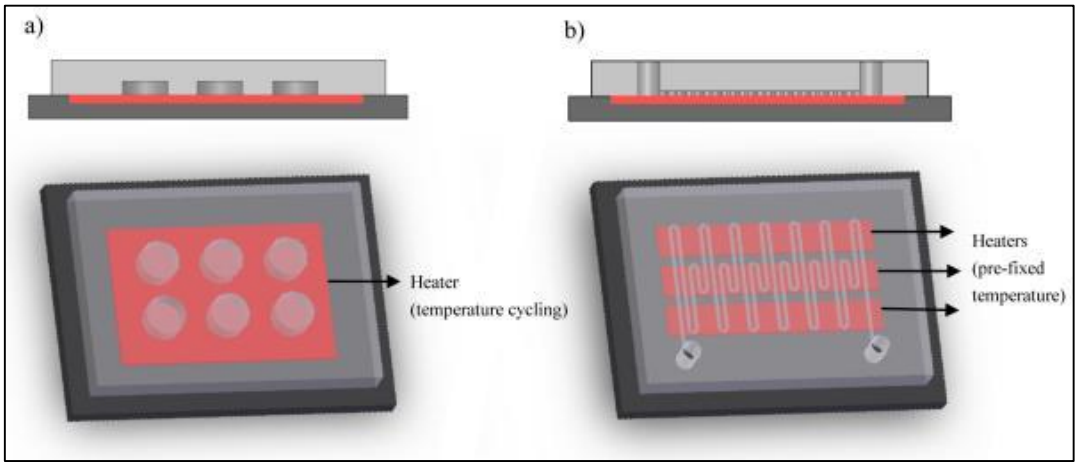

Figure 12: Schematic illustrations of types of microfluidic PCR chip designs. a) stationary chamber system b) continuous flow system. Adapted from [65].

4. Methodology

As was previously mentioned, there is a current need for a viable rapid prototyping method for hard plastics microfluidics. Due to its simplicity, robustness and polymer molding capabilities Hot Embossing was chosen as the basic fabrication technique for a rapid prototyping method. Although much of the existing work in micro-scale Hot Embossing was performed using dedicated machines and labor-intensive molds, there are reports of microfluidic chips fabricated using only a minimal setup with temperature control provided by a hot plate and pressure control with a pre-defined weight [51], for example.

The goal with this experimental work was to develop and test the capabilities of a prototyping system based on a HE minimal setup consisting only of a hot press and a mold. This setup should allow us to fabricate chips with good feature quality (dimensional stability, lack of imperfections, reasonable surface quality, etc); should be reliable and robust, requiring little optimization between different designs and producing identical copies with unchanged parameters; should allow the fabrication of different designs in a short amount of time, requiring both the embossing and the mold fabrication process to be relatively short.

Some initial work was necessary to identify whether this minimal setup was capable of fabricating chips with the required quality or if additional equipment was necessary (dedicated HE machine, automated temperature or pressure control, etc); and to compare mold fabrication methods. After the definition of a working embossing protocol and mold fabrication method the suitability of this setup for rapid prototyping was tested in the development of a PCR chamber microfluidic chip. The goal was to test the developed fabrication setup by iterating on a previous chip design towards an integrated and disposable PCR chip. This example was chosen mainly because it is a non-trivial challenge, with functionality highly dependent on chip design (chamber size, geometry, etc). It was also integrated into other projects in the laboratory so it was possible to leverage the existing knowledge of the PCR process.

The first experiments were focused on testing different hot embossing protocols [20], [23], [32], [37], [54], [55] using different mold materials and fabrication methods. After defining a protocol and CNC Milling as the standard mold fabrication method, PCR chips were designed and fabricated, iterating the design as necessary. CNC Milling was chosen due to its versatility, ease of use and the production of metal molds.

The main goals of the PCR chamber development were to evaluate how fast the fabrication setup could produce a chip with a new design in a reliable way and whether CNC Milling could produce molds with the desired features (minimum feature size, reasonable surface quality, etc). A secondary goal was obtaining in-chip DNA amplification with a simple microfluidic system. The embossing protocol and method continued to be optimized during this process to ease the filling and demolding of deep features. All the designs were embossed both in Polycarbonate (PC) and Cyclic Olefin Polymer (COP) substrates but due to the lack of a suitable sealing method, results were only obtained for PC chips.

The PCR experiments were based on the GeneAmp Fast PCR protocol and the amplification target was the IS6110 gene from M. tuberculosis genomic DNA. All the sample preparation steps were performed off-chip.

Sample preparation protocol:

a) The bench area and all the items needed were bleached beforehand
b) All the reagents were kept on ice
c) 10µL of primer mastermix were made with 1µL forward primer, 1µL reverse primer and 8µL of Nuclease-Free water
d) For each sample to be analyzed, 10 µL PCR mastermix 2x (GeneAmp), 1 µL of primer mastermix and 8.5 µL of Nuclease-Free water were mixed in a 1.5 mL Eppendorf tube to make the PCR mastermix.
e) For each sample, 19.5 µL of PCR mastermix was mixed with either 0.5 µL of TB gDNA (10 µg/mL) or 0.5 µL of Nuclease-Free water, depending on whether it was a positive or negative control.

Gel electrophoresis protocol:

a) 600 mg of agarose was weighed and mixed with 30mL TAE buffer (1x) in an Erlenmeyer flask
b) The flask was covered with Kimwipes and the mixture was repeatedly heated and mixed in a microwave for 30s at a time until the liquid was clear and streak free.
c) The solution was allowed to cool until 60ºC, measured with a thermometer.
d) 3 µL of SYBR Green were mixed with the solution and it was poured on the gel mold, swirling the mold.

e) The gel was covered with foil and left to set for 30 min.
f) After thermocycling the PCR product tubes were put on ice and 10uL of each product was mixed with 2 µL Orange dye.
g) The first well was loaded with 5 µL of DNA ladder and the others with 10 µL of dyed PCR product.
h) The settings used for the electrophoresis were 100V and 50mA and it was ran for 45 min.
i) The gel was placed in a petri dish and covered with foil.
j) The gel was then analyzed using a UV-light imager.

SU-8 mold fabrication Protocol:

a) A Si wafer was placed on the spinner, centered on the spinner chuck, and the vacuum was activated.
b) 2mL of SU-8 3050 photoresist were deposited on the Si wafer.
c) The spinner was ran for 5s at 500 rpm and then for 30 s at 3000 rpm.
d) After turning off the vacuum the coated Si wafer was baked for 15 minutes at 95ºC and then left to cool to room temperature.
e) The wafer was centered underneath a UV lamp and covered with a UV Mask.
f) The setup was then exposed for 30s to UV light.
g) The Si-wafer was then covered with foil and transferred onto a hot plate at 95ºC for 5 min.
h) The wafer was transferred into a dish of SU-8 developer and was gently agitated for 5 minutes and afterwards was rinsed with IPA. This process was repeated until the wafer was cleaned of white residue.
i) The wafer was finally let to dry in air.

PDMS casting protocol:

a) PDMS curing agent and PDMs base were thoroughly mixed on a 1:10 ratio for a total weight of 35g.
b) This mixture was then poured over mold on a Petri dish and placed in a desiccator for 45min.
c) The dish with PDMS was cured in an oven at 75ºC for 1 hour.
d) The PDMS was then peeled off the mold
e) For mold quality studies a ~1mm cross-section was then cut with a blade.

4.1. Materials

The substrate polymers used were PC from McMaster-Carr and COP (ZEONOR 1420R) from Zeon Chemicals, in sheets with different thicknesses from 1mm to 2.5mm. These substrate materials were chosen for their high glass transition temperature, optical clarity, biocompatibility, rigidity, and commercial availability [56], [57].

The designs and molds were drawn using the CAD program SolidWorks 2013 (Dassault Systèmes) and the milling toolpaths were created and exported through the Mastercam X6 for SolidWorks plugin (CNC Software, Inc.).

The metal molds were fabricated using a 3-axis EZTRAK Bridgeport CNC vertical mill and various carbide end mills (Microcut and Harvey Tool) with diameters from 1/4in to 0.002in, depending on the desired features. For tools smaller than 1/8in an Ultra-High-Speed Spindle (Nakanishi HTS1501S-M2040) was used, with a fixed rotation speed of 150 000 rpm, so as to maintain a high cutting speed with a small cutting tool diameter. After milling and the removal of any burrs the molds were sonicated with DI water for 10 mins.

The mold materials tested for CNC milling were MIC 6 Aluminum and C360 Brass (McMaster-Carr). These were selected for their low-cost and availability, good machinability and good thermal properties. MIC 6 Aluminum is cast, presenting very low internal stress and good dimensional stability. It is available as extremely flat plates, preventing the need for extra milling and reducing the fabrication time. C360 Brass is also called free-cutting or free-machining brass due to its extremely good machinability. It has a small percentage of lead which acts as lubricant during milling, eschewing the need for lubricant while producing small chips. For other metal pieces 6061 Aluminum (McMaster-Carr) was used due to its rigidity and low-cost.

In the photolithography-based mold fabrication, SU-8 3050 (Microchem) was spun on Silicon wafers and exposed to UV light through patterned masks. After development, the patterned silicon wafers were then used directly as the HE molds.

The hot embossing itself was performed using a manual press (Model C 3851 Carver) with manually controlled aluminum heated platens (2101 Carver). The pressure and temperature was monitored by reading the force and temperature gauges.

The embossed chips were cleaned with DI water, Isopropanol, DI water, and Ethanol (Thermo Fisher Scientific) and dried with compressed Nitrogen.

5. Results and Discussion

5.1 Testing Hot Embossing protocols and mold fabrication methods

The first Hot Embossing experiments were performed on a PC substrate using a previously machined aluminum mold (Figure 13). This was used to test different protocols, changing embossing temperature, embossing time, embossing pressure and demolding temperature. The temperature was controlled using a thermostat on each platen, the pressure was manually controlled, and demolding was performed by hand.

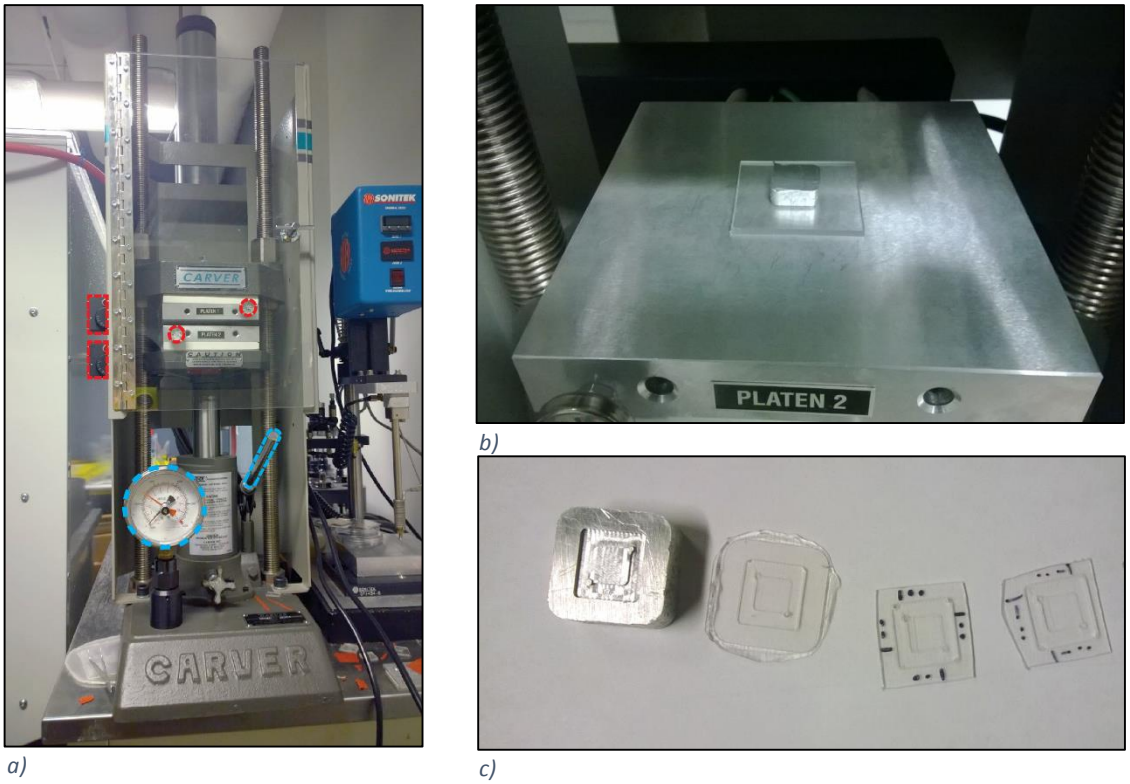

a) b) c)

Figure 13: Hot Embossing Equipment: a) Hot press with temperature (red) and pressure (cyan) controls; b) Aluminum mold on the PC substrate before embossing; c) Aluminum mold with embossed pieces.

After some testing it was possible to heat up to the embossing temperature on each platen without overshooting the target in under 10 minutes. By turning the heaters on/off as necessary is was possible to maintain a constant temperature (+/- 1.5 ºC). The cooling down was passive, with the heaters turned off. Depending on the embossing and demolding temperatures the cooling down usually took anywhere from 20 min to 30 min.

As expected the minimum embossing temperatures were around 15 ºC above glass transition temperature of PC (146ºC). Chips embossed at lower temperatures presented low optical clarity and incomplete filling of some features. Embossing pressure used was around 22MPa as the minimum force possible was around 500 pounds-force and the mold had an area of 10mm x 10 mm. The exact pressure value was found to not be a critical parameter, as long as it remained constant.

One interesting find was the importance of the rate of pressure increase, from contact pressure to embossing pressure, something rarely mentioned in the literature. A slow rate (0->P_e in 60s) was found to produce substantially better feature filling. Another important fact was the difficulty in separating the mold from the piece after embossing (demolding), most likely due to the high vertical walls of the mold. Although mentioned in the literature, this problem is usually minimized as the features embossed are shallower, with smooth surfaces (LIGA, etc), and therefore present lower adhesion forces between the mold and the piece. One common solution to this problem is the use of a release agent between the mold and the substrate but this adds to the duration and complexity of the embossing process

SU-8/Silicon molds were also tested using identical protocols but were found to be extremely fragile and would often break during embossing and demolding (Figure 14). The features (straight channels 100-500 µm wide, 100 µm deep) were embossed with good quality, presenting no defects. The good embossing quality makes SU-8/Silicon molds a feasible alternative to CNC Milled molds, as it allows for the use of designs, knowledge and equipment developed for SL. In a rapid prototyping scenario this setup presents some limitations as it will be hard to obtain a reasonable number of copies (>3) from the same mold and design changes become dependent on the time it takes to obtain a UV-mask with a new design (usually over 24h).

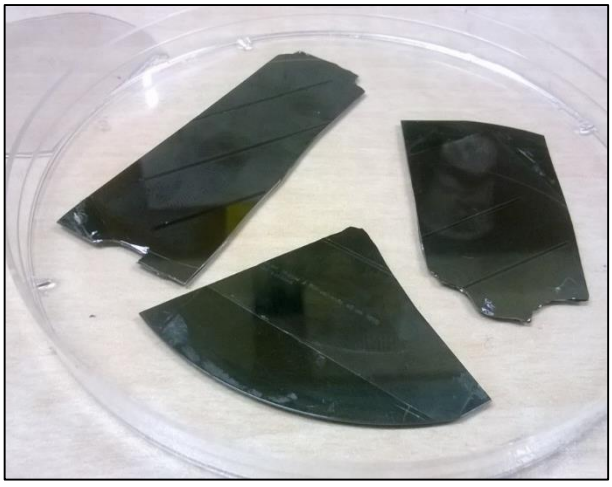

Figure 14: Pieces of a broken SU-8/Silicon mold.

In order to test the minimum resolution possible with CNC Milling and minimal setup HE, a test mold with straight channels (50 µm channels 50 µm apart, 100 µm channels 100 µm apart and 150 µm wide channels 150 µm apart) was designed and milled in aluminum. As this was the first contact with Micro Milling, there were some problems in the fabrication: the milled channels were narrower than desired, presented rough walls, the depth of the channels wasn't consistent between thinner and wider channels and the milling tool used was damaged during fabrication. After troubleshooting, it was found that there were some errors in the toolpath definition, the DOC and feedrate hadn't been properly adjusted to account for the high rotational speeds and small diameter and that precise calibration of the Z-axis between each tool change was critical. The milling quality was tested through visual inspection of the molds and of cross-sections obtained through PDMS casting (Figure).

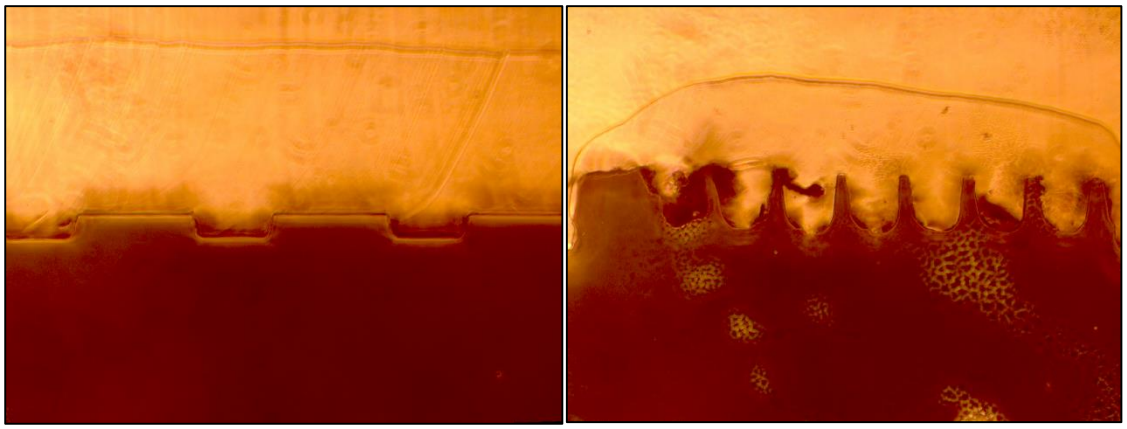

Figure 15: Cross-sections of the milled channels obtained through PDMS casting. Left- wider channels (150 µm design). Notice the smooth walls and shallow depth of cut. Right – Thinner channels (50 µm design). Notice the deep, milled features and the thin standing ones.

The embossing process was successful, reproducing the milled features as expected (Figure 16). It was useful to notice that even thin and deep mold features were filled and successfully embossed.

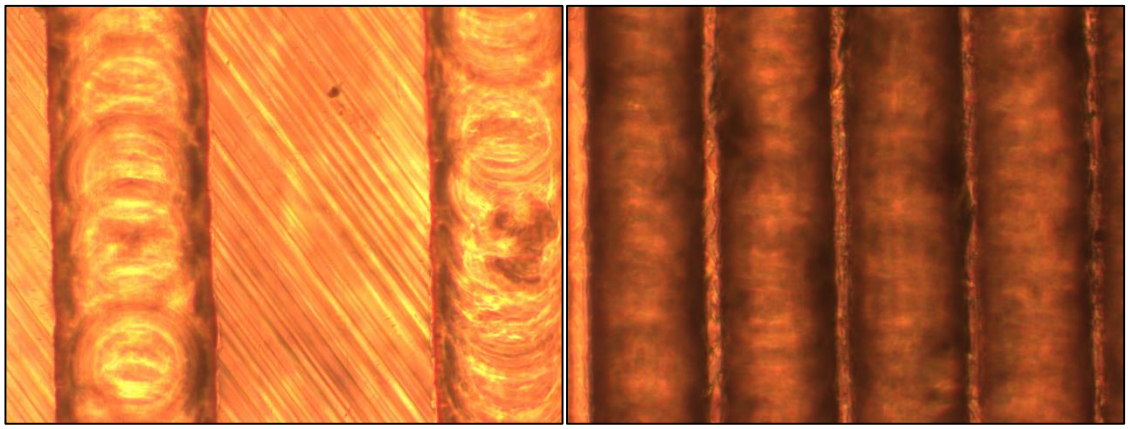

Figure 16 : Embossed PC chip. Left- wider channels (150 µm design). Right – Thinner channels (50 µm design). Notice the accurate embossing of all the features, including the characteristic machining texture.

A second test mold was designed with meandering channels 120 µm wide. The goal was to test the embossing and fabrication of more complex features. The chip was designed so it would only be necessary to use a single milling tool (0.004' diameter), to avoid having to re-calibrate the z-axis. Although the embossing was again largely successful there were some problems with milling (Figure 17). The mold channels presented some defects and were not identical in width. This was later found to be due to the small distance between toolpaths (<5 µm) which the CNC mill approximated to increments of around 3 µm, its minimum resolution. Another source of error was the slow feedrate which although usually recommended to obtain a better surface finish can cause irregular cuts and damage the cutting tool, as was the case.

During this process it was also discovered that brass molds were unsuitable for embossing PC chips as the final chip had defects (bubbles and rough surfaces) not present when embossing with otherwise identical (same surface quality, same features) aluminum molds. It would be desirable to use free-cutting brass as a mold material due to its lack of need for lubricant during machining. Since this defects were not present when embossing COC chips with the brass molds and that a thin residual layer formed on the brass mold when embossing with PC, it was hypothesized that there was a reaction happening between the PC substrate and the brass. After careful examination it was found that one of the common components of PC, chlorobenzene, is corrosive to brass at embossing temperatures. With that in mind the material used for all the molds in this work was aluminum.

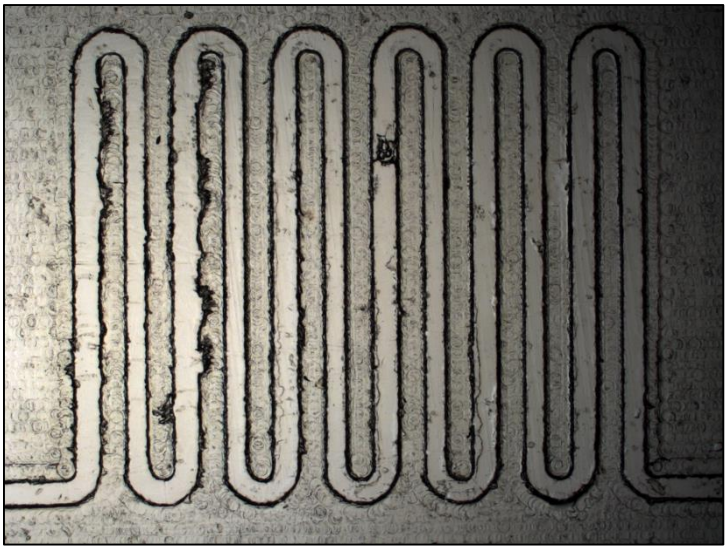

Figure 17: Meandering channels 120 µm wide. Notice the different widths on the right and left channels and the uncut areas on some regions.

5.2 Development of a hard polymer PCR chip

In order to test the practicality of using HE for microfluidic fabrication it was used in the development of a PCR microfluidic chip. The work began with using a previously tested design and adapting it to create a HE mold. The previous design had been fabricated by CNC milling directly on a PC substrate (Figure 18) and the SolidWorks (SW) drawings were adapted to build a HE mold. This design was tested, optimized and tested again. The design was changed multiple times using the developed prototyping workflow and it was possible to obtain PC chips of each design in under 6h.

The initial setup consisted of a reaction chamber and a temperature sensing chamber in a PC square chip, with an external thermoelectric heater placed under the chip. The reactions chamber was filled with the PCR reagents and the sample, with the temperature sensing being performed by a thermistor (Custom Electric). The chambers were sealed using acetonitrile and 120µm thick PC film and the inlets were sealed using adhesive tape. The heater was controlled with a simple ON/OFF feedback mechanism controlled by an Arduino UNO microcontroller with input from the thermistor. The temperature was monitored on a computer monitor connected to the microcontroller as well. The goal was to thermocycle the sample in order to obtain DNA amplification and to calibrate the system so that in the future only external sensing would be necessary.

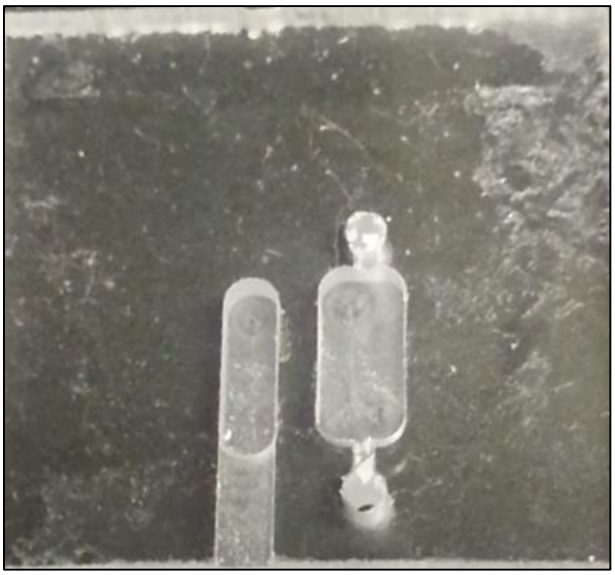

Figure 18: PCR chip with features directly milled on the PC substrate

It was hypothesized that the poor results (lack of amplification) obtained using the CNC milled chips were due to the rough surface finish on the PC chip (see Figure 18), which caused too much protein adsorption during the reaction. Milling a HE metal mold instead of milling the plastic directly would improve the surface quality of the chamber dramatically. The only change in the design was the increase in the distance between the reaction chamber and the temperature sensing chamber to accommodate for the size of the smallest endmill available (1/16'') (see Figure 19). Care was taken so that both chambers would still be on top of the heater, roughly a 6.3cm x 8.25cm rectangle.

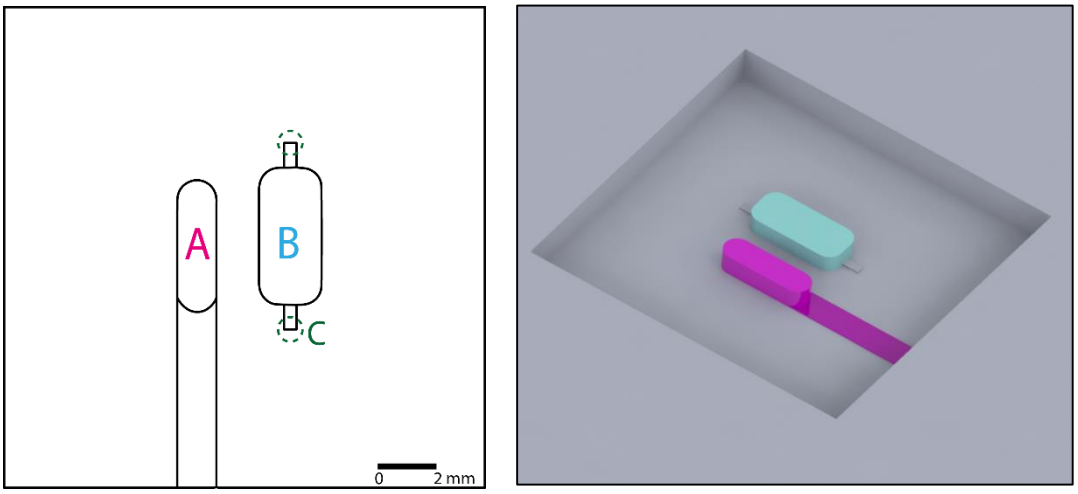

Figure 19: First mold design with a temperature sensing chamber (A/purple) and a reaction chamber (B/cyan). The inlets were drilled after embossing on the sites marked (C).

Based on the previously described work the first HE parameters used were an embossing temperature (T_e) of 160ºC, an embossing pressure (P) of 22 MPa and an embossing time (t_e) of 10 min. The demolding was performed at 115ºC (T_d) using pliers and a screwdriver. To get a good feature filling the substrate piece was cut to size so that the pressure was applied mostly on the chip area.

After several tries to optimize the embossing process the parameters used were T_e=176ºC, P=11 Mpa, t_e=15mins and T_d=140ºC. The higher embossing temperature and lower pressure were used to introduce less stress into the chip. The pressure increase – from 0 to 11 MPa – was not immediate and was instead performed over 60 seconds to allow for the plastic to fill the mold cavity. The longer embossing time was used to allow for a complete filling of all features and also to reduce the thickness of the residual layer. The higher demolding temperature was used to diminish the adhesion force during demolding and ease the demolding process. Another change was the use of a glass slide between the substrate and the top platen so as to create a smooth surface on the unfeatured side of the chip (see Figure 20).

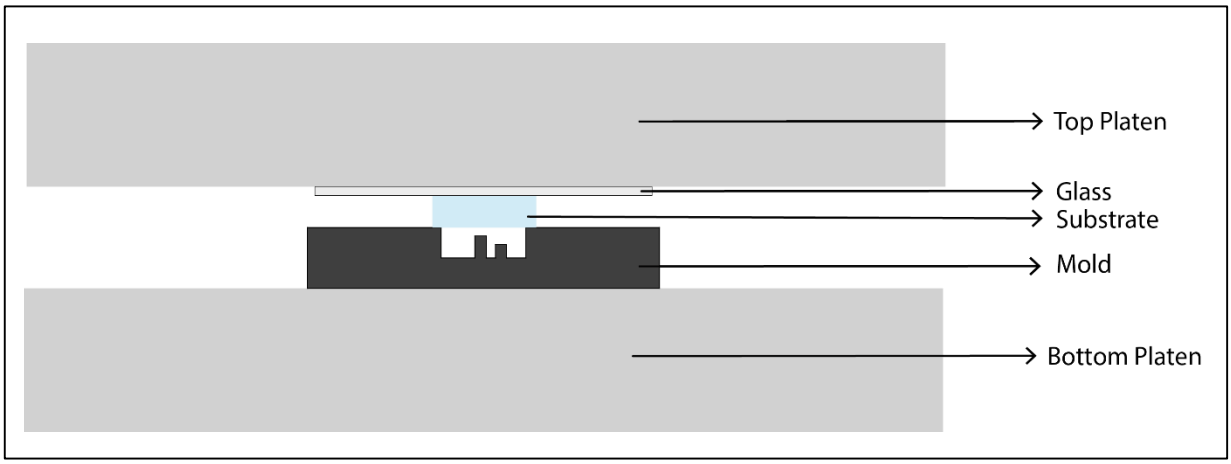

Figure 20: Diagram of embossing setup. Both the top and bottom platens were heated and had integrated temperature sensors. Notice the glass slide between the substrate and the top platen.

Despite the higher T_d, demolding was still a problem due to the long and deep vertical walls which created strong adhesion forces. In order to ease the demolding process a perforated metal shim (0.5mm thick) was placed between the substrate and the mold during embossing. The demolding was then performed by removing the metal shim which pulled the piece out of the mold. The inlets (C) were milled directly on the chip with a 1mm mill on a drill press. The chips were cleaned with DI water, IPA, ethanol and DI water again and dried with compressed Ni.

5.2.3. PCR experiments

After optimizing the embossing parameters, 3 identical copies were embossed as described above. A PCR experiment was set up with a negative and a positive control off-chip – the thermocycling was conducted in a conventional thermocycler - and 3 different on-chip experiments. The sample used was M. tuberculosis genomic DNA and the amplification target was the IS6110 gene. The on-chip experiments were designed to try to pinpoint possible failure points along the process. One sample was placed on-chip for 5 minutes with no thermocycling, a second was thermocycled for only 5 minutes, and a third went through the full thermocycling (35 cycles). The thermocycling was done according to a Fast PCR Protocol (GeneAmp Fast PCR) with only two temperature steps.

For thermocycling the chips were filled with the PCR reagent mix using a micropipette and sealed with adhesive tape for the required duration. The sealed chip was placed on top of the heater and fixed in placed with the help of a milled PC piece and two binder clips. All the samples were tested at the same time using gel electrophoresis.

As can be seen in Figure 21, no amplification was detected in any of the on-chip samples. It was hypothesized that this might have been due to the surface roughness of the inlets causing protein adsorption, as these were machined after embossing the chip

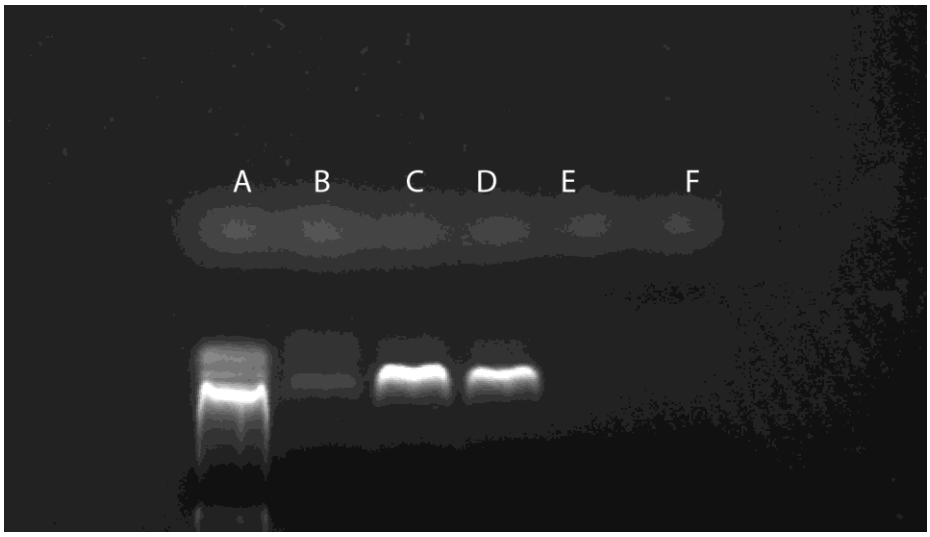

Figure 21: PCR amplification results obtained through gel electrophoresis. A- DNA ladder; B- Negative Control; C- Conventional thermocycling; D – Conventional thermocycling with 5 min incubation on-chip; E- 5 min on-chip thermocycling + conventional thermocycling; F – On-chip thermocycling only. Only the existence of amplification was being tested.

In order to eliminate any post-embossing machining, a new mold which incorporated the inlets was designed and milled. Another minor change was the increase in depth of the thermistor wires' cavity. Although the parameters used were the same as the previous mold, it was not possible to get a good filling and easy demolding at the same time. After experimenting with different parameters and still not obtaining satisfactory results the mold setup was changed.

A "two part" mold (Figure 22) was developed so that the strong adhesion forces around the chip would help the demolding process instead of hampering it. The top part of the mold was CNC milled on 2mm thick stock Aluminum sheet with room for the chip features (20mm x 20mm, in orange) and alignment features (green). The bottom part was CNC milled and included both the chip features (inlets - red, reaction chamber - cyan, thermal chamber - purple) and the alignment features (dark blue). This setup allowed for the use of different bottom chip designs while maintaining the same top part. The demolding was done by separating the top and the bottom parts by hand using sheepskin gloves and pliers.

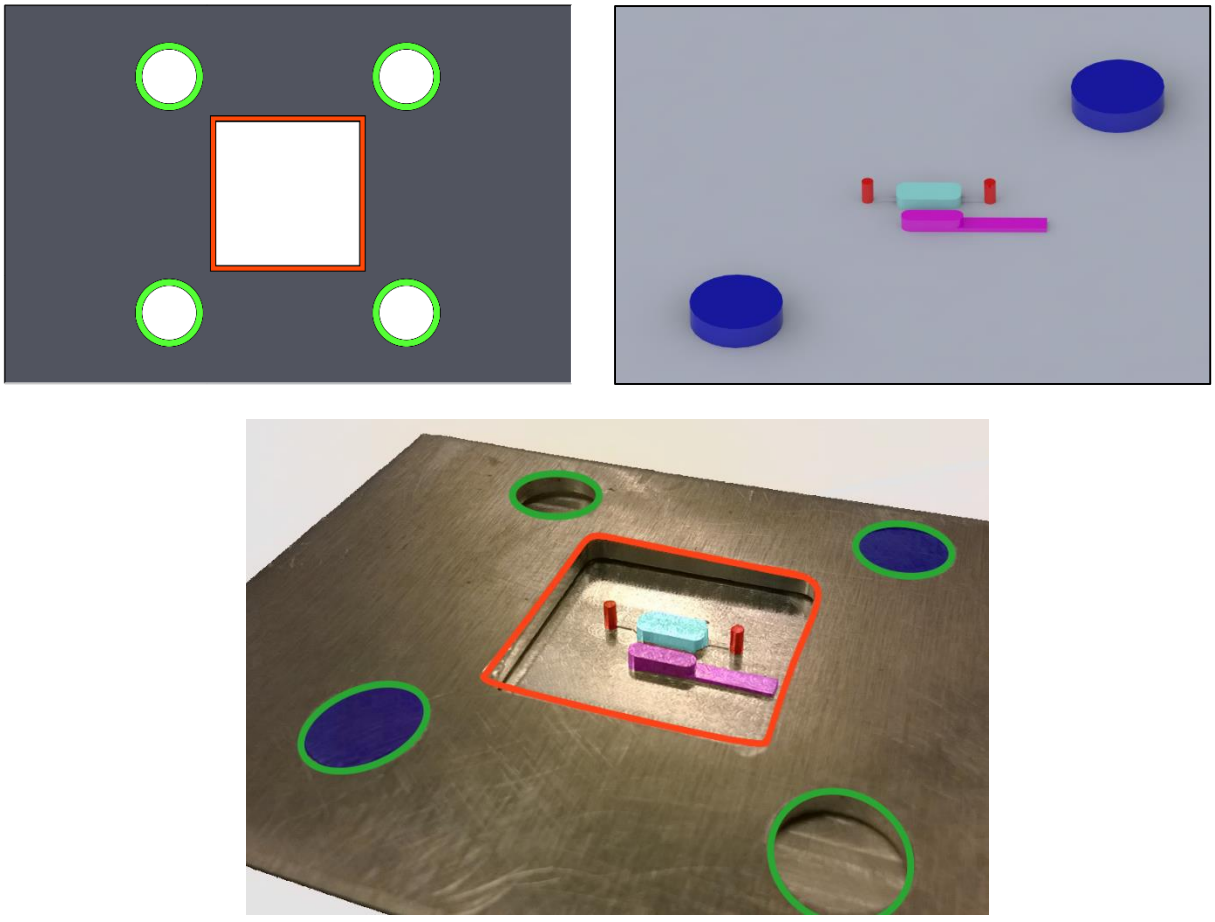

Figure 22: Two part mold. a) Top part with a 20 x 20mm square (orange) defining the chip size and alignment features (green). b) Bottom part with chambers, inlets and alignment features (dark blue). c) Assembled two part mold with color highlights

By using this setup it was possible to obtain good chips, with no problems in filling or demolding. It was also much easier and faster to demold after removing the piece from the hot press. This setup also allowed for different chip designs while maintaining the same chip dimensions.

Five more chips were produced and sealed and the experiment was ran with an identical protocol to the previous one. The results were the same as before with no DNA amplification detected in chips where heating occurred.

Having ruled out surface roughness as the main problem and after reviewing the design, temperature control was pinpointed as the most likely point of failure - the thermistor was found to be far from an ideal temperature sensor, as it was not in contact with water or other similar liquid; it was relatively slow reacting; and it had a large mass which could complicate the calibration afterwards.

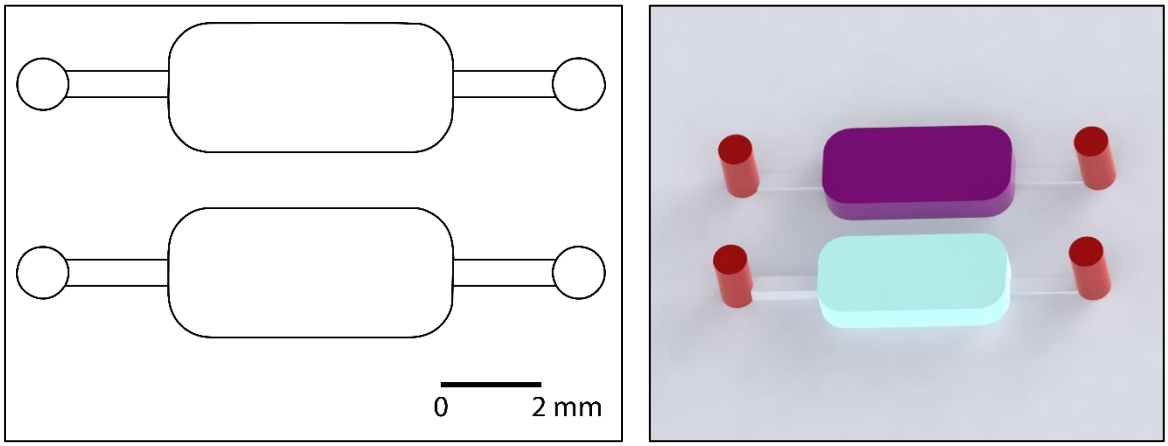

Figure 23: Two chamber design. Inlets – red; reaction chamber – cyan; thermal chamber – purple.

With that in mind a new design was proposed and tested (Figure 23). It consisted of two identical chambers side by side with one being the reaction chamber and the other the temperature sensing chamber. The temperature sensing would be performed by a small thermocouple (Custom Thermoelectric) instead of the thermistor due to its much smaller size and faster response. During preliminary testing this design presented some issues, mostly integrating the thermocouple into the chamber while maintaining good sealing between the chip and the film. It was also discovered that there were large temperature differences inside the chamber. During heating the temperature at the bottom of the chamber, in contact with the heater, was considerably hotter than at the top. This also produced the secondary effect of some regions of the chamber taking a long time to reach the target temperatures.

To avoid this phenomenon a new design was proposed (Figure 24). The main requirements were to maximize the contact area between the chamber and the heater and to minimize the height of the chamber, while maintaining a minimum volume (8-10µL). The positioning and shape of the inlets and corners was also taken into consideration to try to minimize bubble formation. The chip was also made thinner (1 mm vs 2 mm) to decrease the thermal mass of the chip. With the new design it became impossible to measure the temperature inside the chamber during the thermocycling as any thermal sensor might interfere with the PCR reaction. The solution to this was to calibrate the temperature on the outside of the chamber (on top of the heater) with the temperature inside and then use only the outside temperature.

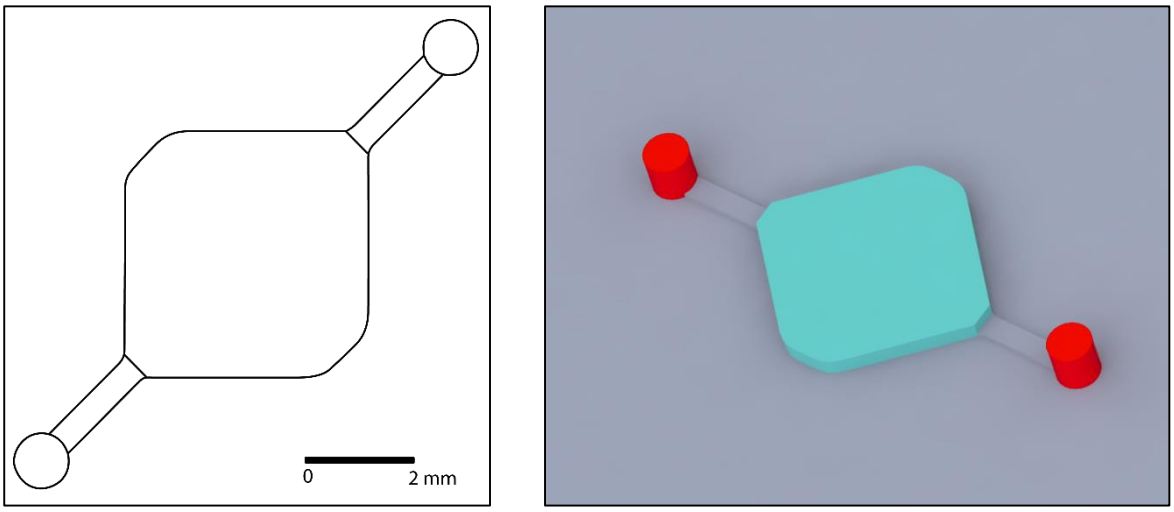

Figure 24: Single Chamber Design. Single reaction chamber (cyan) with inlets (red). The chamber dimensions are 4.5 x 4.5 x 0.4 mm.

A thermocouple was integrated into the chip during embossing (see Figure 25). The thermocouple tip was placed on top of the reaction chamber mold during hot embossing and became embossed into the chip, under the reaction chamber. The material between the thermocouple tip and the bottom of the chamber was removed and the tip raised to allow for it to come in contact with the chamber contents. Care was taken not to remove too much material and to leave the surface as undamaged as possible.

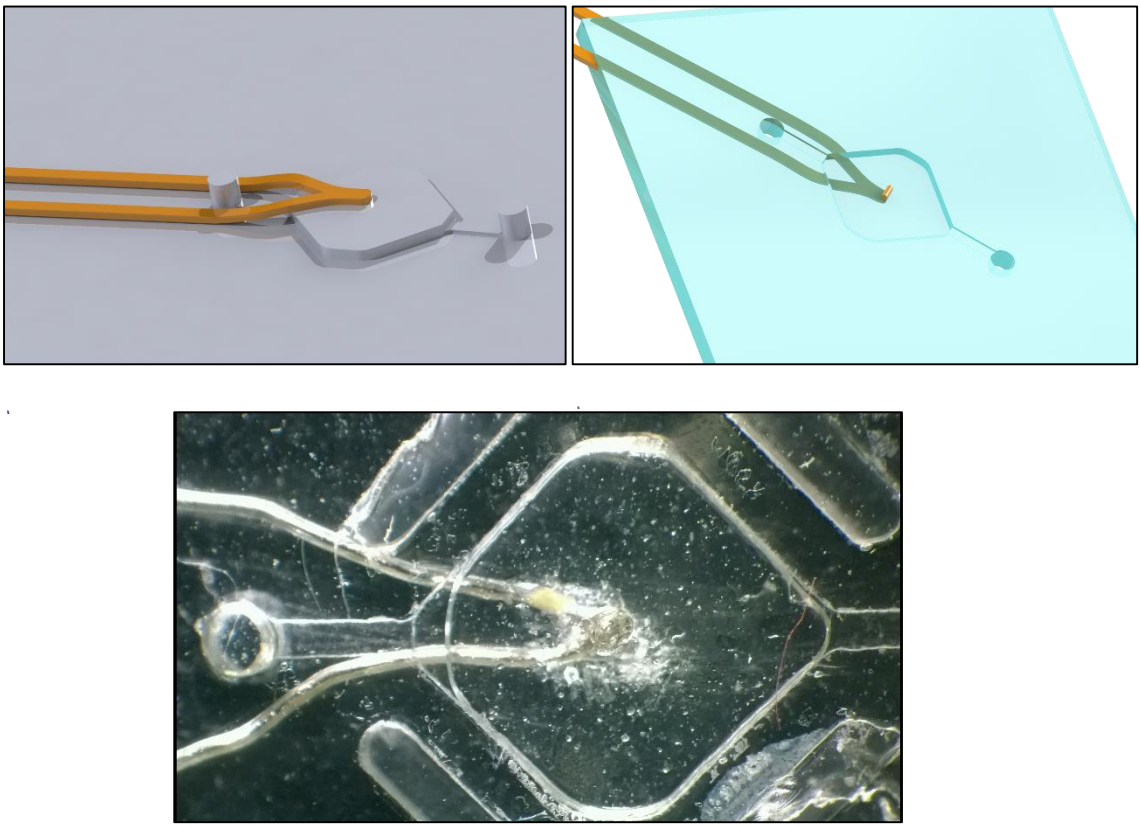

Figure 25: Integration of a thermocouple in the reaction chamber. a) Diagram of the thermocouple on top of the chamber mold before embossing. b) Diagram of the thermocouple integrated on the chip, with the tip inside the reaction chamber. c) Photograph of a thermocouple tip integrated in a chip. Notice the roughness around the thermocouple tip.

During temperature measurement it was found that the relationship between the temperatures measured inside and outside was highly dependent on the relative positions of the heater, reaction chamber and outside thermocouple. To solve this problem a piece was designed to hold all the elements in a well-defined, fixed position. The first step was defining the position of the external thermocouple on the heater surface. It was defined as close as possible to the heater border to leave room for the reaction chamber while avoiding the border itself, where the surface temperature is more inhomogeneous. The thermocouple was fixated on the heater border with a thermally conductive tape. The second step was to fixate the chip position relative to the heater. This was done by designing and 3D printing a holder with alignment features and room for the thermocouple's and the heater's wires. This allowed for a good contact between the chip and the heater and for different chips to be used, always in the same position relative to the heater and thermocouple (see Figure 27).

With this in mind the chip design was updated (Figure 26) to incorporate the alignment features and to create an indentation for the external thermocouple. Another addition were the thermal guards around the reaction chamber which function as insulators and help position the thermocouple tip. The thermal guards were positioned as close to the reaction chamber as the mills available would allow.

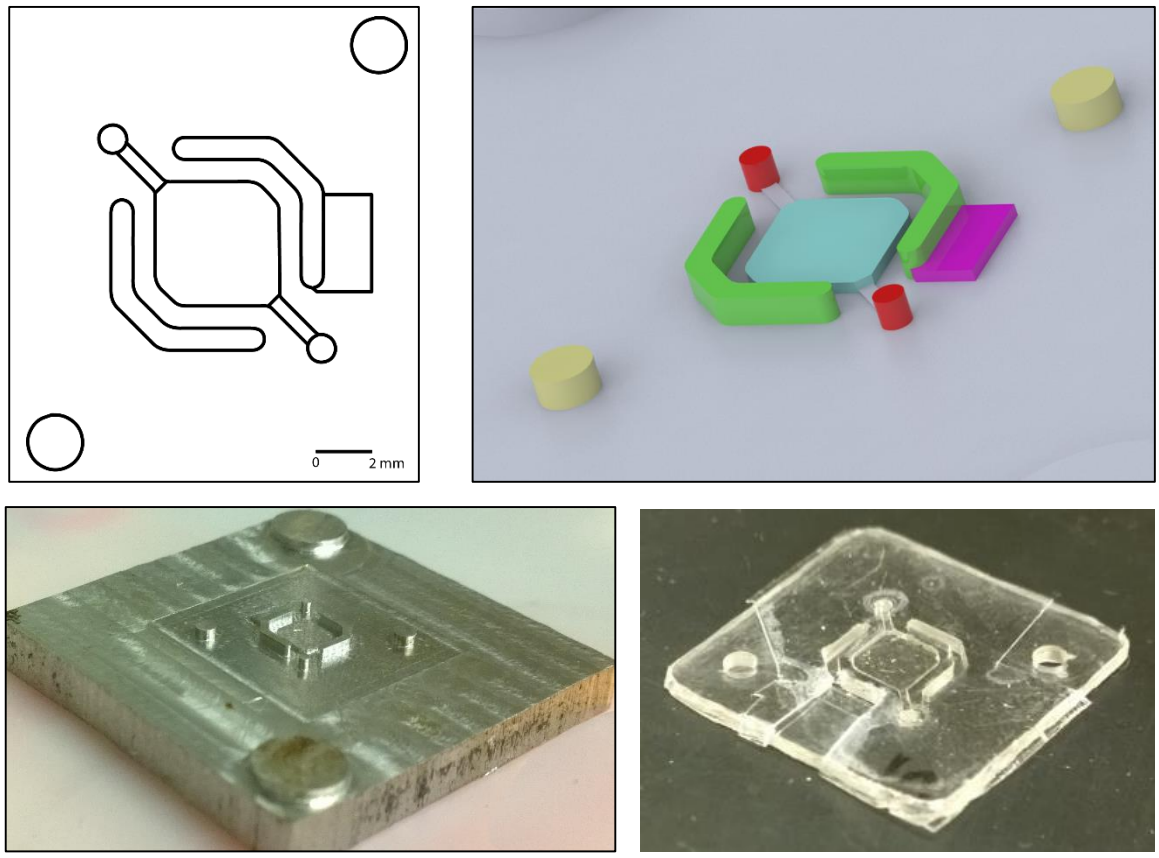

Figure 26: Second Single Chamber Design. a) Single chamber design viewed from the top. b) 3D view of a SW model of the mold. Reaction chamber – cyan; Inlets – red; thermal guards – green; thermocouple indentation – purple; holder alignment features – yellow. c) CNC milled aluminum mold bottom part. Notice the different finish quality depending on the mill used for each site. d) Sealed PCR chip.

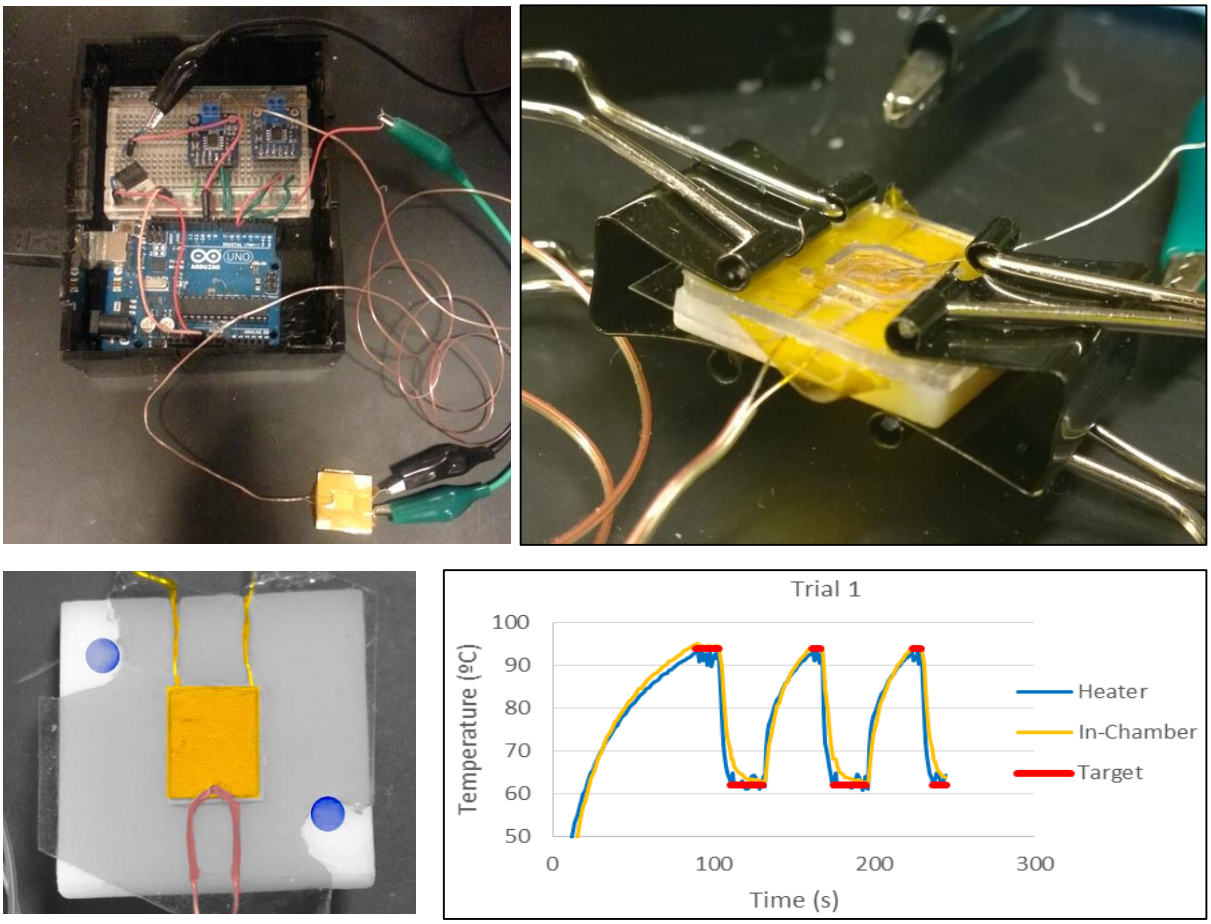

Figure 27: a) Thermocycling setup with the temperature control circuit and the heater holder; b) Chip and holder setup during thermal calibration. Notice the binders and the contact between the chip and the holder; c) Heater holder with features highlighted. Heater – yellow, Thermocouple – red, Chip alignment features – blue. d) Temperature profile during a calibration run. Notice the difference between target temperature and in-chamber temperature on the lower 62

Temperature Calibration

As was mentioned above, during the first temperature calibration tests there was a large variation (>20ºC) between the temperatures measured outside and inside the reaction chamber. This was mostly due to variations on the external thermocouple position and the lack of good contact between the chip and the heater. After building the heater holder and defining the external thermocouple position on the heater it was possible to calibrate the system. This was done by changing the target temperature of the controller program (measured on the surface of the heater) so that the in-chamber temperature would match the targets of 94ºC/62ºC (see Figure 28).

In order to test the reliability of the calibration, the chip was emptied and refilled with water and the thermocycling protocol was ran for a few cycles with the calibrated parameters. The in-chamber temperature was found to be within 1ºC of the target temperature at all temperature levels. The calibration was tested again by embossing a completely new chip and repeating the same protocol. The results were identical to the previous ones, with the temperature remaining within 1ºC of the target.

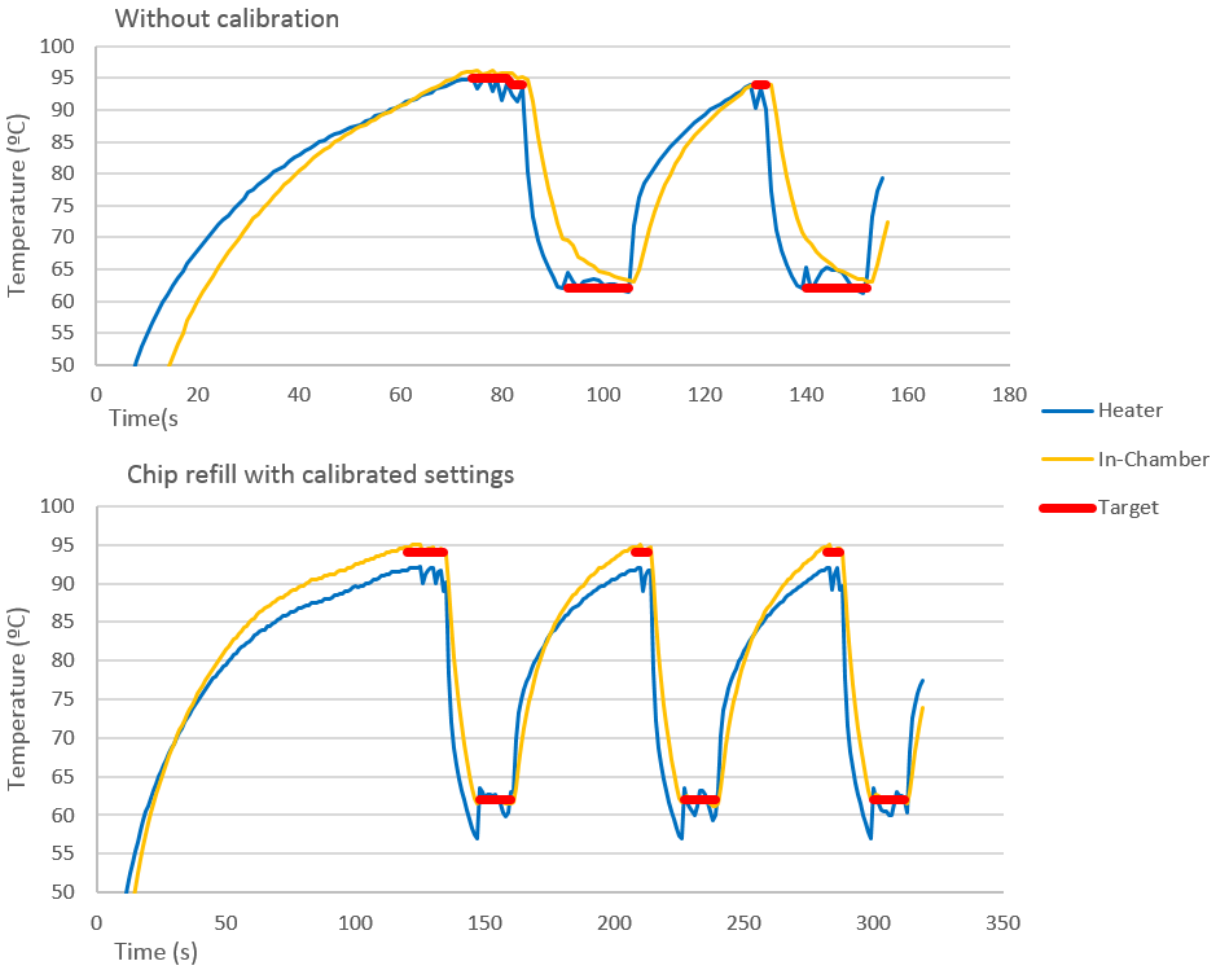

Figure 28: Temperature profile of both thermocouples during thermocycling. The top profile shows the first results obtained with the target temperature in the program equal to the desired temperature. The bottom profile shows the results obtained after calibration and refilling the chip. Notice the low variation of the in-chamber temperature.

Although it was not the scope of this work, it is interesting to note that the heating (0.5ºC/s) and cooling (1.3ºC/s) rates are comparable to commercial thermocyclers. Based on the literature on PCR miniaturization this measure is expected to improve with thermal optimization in the future.

Bubble Formation

After the temperature calibration, the PCR experiment was ran again, with identical results to previous experiments. During the thermocycling it was noticed that several air bubbles appeared inside the chamber (see Figure 29: Bubble formation during thermocycling. The chip was filled with colored water to test bubble formation.Figure 29). These appeared as small bubbles concentrated around the chamber walls during the first thermal cycles but grew during the thermocycling protocol eventually filling the chamber. This presented a major obstacle as bubbles cause temperature inhomogeneity and increase the pressure inside the chamber, removing the sample from the chamber into the inlets [42]. Bubble formation is a common problem in microfluidic PCR systems as the high temperature causes any micro-bubbles present to expand with each thermal cycle. These micro-bubbles can be introduced during sample loading, chip sealing or be already present in the sample [58]. Due to the initial location of the bubbles it was hypothesized that air was being trapped on the chamber walls during sealing. The sealing method was optimized - applying the solvent using a brush instead of pipetting and immediately absorbing excess solvent; and applying pressure directly on the chamber walls and around the inlets. This produced some results as the bubbles took longer to appear and grow but throughout an entire thermocycle (~35 cycles) they would still fill the chamber.

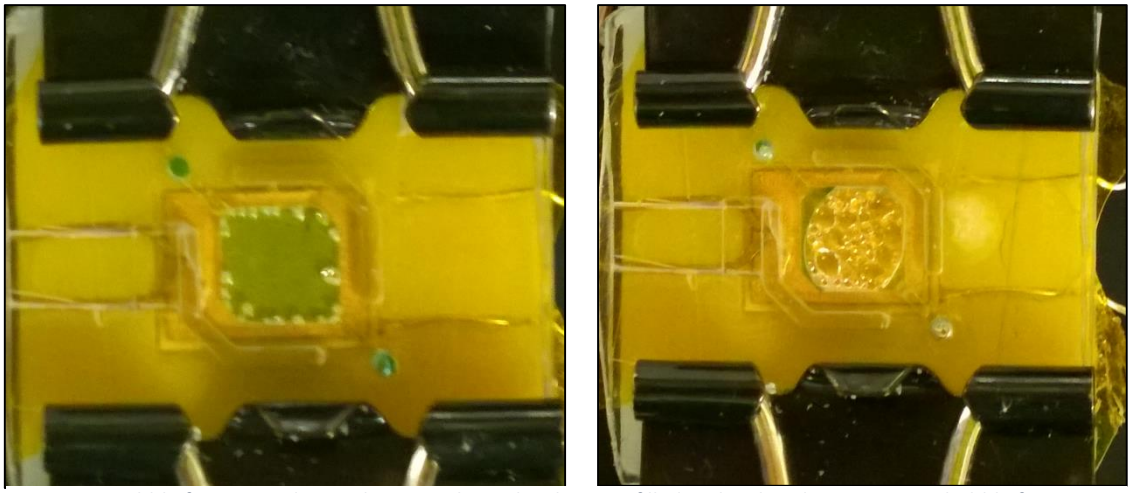

Figure 29: Bubble formation during thermocycling. The chip was filled with colored water to test bubble formation.

In the current system, bubble formation is suspected to be the major impediment to a successful PCR amplification reaction. Although there are some solutions to this problem in the literature, only a few are applicable to a hard plastic POC system – geometry optimization and surface modification. It has been reported that different chamber shapes [59], depths [58] and hydrophobicity [59], [60] can greatly influence bubble formation.

6. Conclusion

My goal with this work was to develop a way to prototype hard plastic microfluidics in a fast and simple way. I began by identifying the methods better suited for this task, with special focus on simplicity and similarity with industrial production methods. Hot Embossing was selected as the basic fabrication method as it presents good reproduction quality and produces results similar to Injection Molding with minimal optimization.

After performing some preliminary experiments with different mold fabrication methods and Hot Embossing protocols, I defined a simple rapid prototyping protocol based on CNC Milling and Hot Embossing for Polycarbonate microfluidics. This protocol was then optimized and tested through the development of a microfluidic PCR chamber.

As expected, this presented many challenges and required extensive design changes throughout the process. This allowed me to test the prototyping protocol in a demanding situation, with specific design goals and requirements.

Overall, the main conclusion I draw from this work is that Hot Embossing is an excellent platform for prototyping microfluidics and that it is possible to prototype microfluidic devices in hard plastic in a laboratory setting. The developed protocol allowed for rapid fabrication of new designs, easily producing multiple identical copies in under 8h.

POC devices have tremendous potential in the medical field. If successful, they could allow for new paradigms of medical data acquisition, either enabling home-use monitoring or allowing for comprehensive medical testing in resource-poor settings, for example. For this possibility to become a reality, these devices need to be disposable and durable and at the moment this can only be achieved using hard plastics. I expect that by having worked towards a simple and inexpensive prototyping method for hard plastics it will be easier to produce functional POC devices with real-world applications.

7. Bibliography

[1] N. Nguyen and S. Wereley, *Fundamentals and applications of microfluidics*, 2nd ed. ARtech, 2006, p. 497.

[2] A. Manz, N. Graber, and H. M. Widmer, “Miniaturized total chemical analysis systems: A novel concept for chemical sensing,” *Sensors Actuators B Chem.*, vol. 1, no. 1–6, pp. 244–248, Jan. 1990.

[3] Y. Xia and G. M. Whitesides, “SOFT LITHOGRAPHY,” *Annu. Rev. Mater. Sci.*, vol. 28, no. 1, pp. 153–184, Aug. 1998.

[4] G. M. Whitesides, E. Ostuni, S. Takayama, X. Jiang, and D. E. Ingber, “Soft lithography in biology and biochemistry.,” *Annu. Rev. Biomed. Eng.*, vol. 3, pp. 335–73, Jan. 2001.

[5] K. Erickson and P. Wilding, “Evaluation of a novel point-of-care system, the i-STAT portable clinical analyzer,” *Clin. Chem.*, vol. 39, no. 2, pp. 283–287, Feb. 1993.

[6] E. Sollier, C. Murray, P. Maoddi, and D. Di Carlo, “Rapid prototyping polymers for microfluidic devices and high pressure injections.,” *Lab Chip*, vol. 11, no. 22, pp. 3752–65, Nov. 2011.

[7] S. K. Sia and G. M. Whitesides, “Microfluidic devices fabricated in poly(dimethylsiloxane) for biological studies.,” *Electrophoresis*, vol. 24, no. 21, pp. 3563–76, Nov. 2003.

[8] K. Y. Lee, “Micromachining applications of a high resolution ultrathick photoresist,” *J. Vac. Sci. Technol. B Microelectron. Nanom. Struct.*, vol. 13, no. 6, p. 3012, Nov. 1995.

[9] H. Lorenz, M. Despont, N. Fahrni, N. LaBianca, P. Renaud, and P. Vettiger, “SU-8: a low-cost negative resist for MEMS,” *J. Micromechanics Microengineering*, vol. 7, no. 3, pp. 121–124, Sep. 1997.

[10] A. Mata, A. J. Fleischman, and S. Roy, “Characterization of polydimethylsiloxane (PDMS) properties for biomedical micro/nanosystems.,” *Biomed. Microdevices*, vol. 7, no. 4, pp. 281–93, Dec. 2005.

[11] H. Wu, T. W. Odom, D. T. Chiu, and G. M. Whitesides, “Fabrication of complex three-dimensional microchannel systems in PDMS.,” *J. Am. Chem. Soc.*, vol. 125, no. 2, pp. 554–9, Jan. 2003.

[12] U. M. Attia, S. Marson, and J. R. Alcock, “Micro-injection moulding of polymer microfluidic devices,” *Microfluid. Nanofluidics*, vol. 7, no. 1, pp. 1–28, Feb. 2009.

[13] J. Giboz, T. Copponnex, and P. Mélé, “Microinjection molding of thermoplastic polymers: a review,” *J. Micromechanics Microengineering*, vol. 17, no. 6, pp. R96–R109, Jun. 2007.

[14] J. Giboz, T. Copponnex, and P. Mélé, “Microinjection moulding of thermoplastic polymers : from theory to experiment,” in *Proceedings of the 3rd International Conference on Multi-Material Micro Manufacture*, 2007, p. 4.

[15] R. Surace and G. Trotta, “The micro injection moulding process for polymeric components manufacturing,” *New Technol. – Trends, Innov. Res.*, 2012.

[16] C. Zhang, J. Xu, W. Ma, and W. Zheng, “PCR microfluidic devices for DNA amplification.,” *Biotechnol. Adv.*, vol. 24, no. 3, pp. 243–84, Jan. 2006.

[17] R. K. Jena, C. Y. Yue, Y. C. Lam, and Z. Y. Wang, “High fidelity hot-embossing of COC microdevices using a one-step process without pre-annealing of polymer substrate,” *Sensors Actuators B Chem.*, vol. 150, no. 2, pp. 692–699, Oct. 2010.

[18] E. W. Becker, W. Ehrfeld, P. Hagmann, A. Maner, and D. Münchmeyer, “Fabrication of microstructures with high aspect ratios and great structural heights by synchrotron radiation lithography, galvanoforming, and plastic moulding (LIGA process),” *Microelectron. Eng.*, vol. 4, no. 1, pp. 35–56, May 1986.

[19] L. Peng, Y. Deng, P. Yi, and X. Lai, “Micro hot embossing of thermoplastic polymers: a review,” *J. Micromechanics Microengineering*, vol. 24, no. 1, p. 013001, Jan. 2014.

[20] M. Worgull, “Hot Embossing Process,” in *Hot Embossing : Theory and Technology of Microreplication*, 2009, pp. 137–177.

[21] Y. He, J.-Z. Fu, and Z.-C. Chen, “Optimization of control parameters in micro hot embossing,” *Microsyst. Technol.*, vol. 14, no. 3, pp. 325–329, Dec. 2007.

[22] J.-T. Wu, S.-Y. Yang, W.-C. Deng, and W.-Y. Chang, “A novel fabrication of polymer film with tapered sub-wavelength structures for anti-reflection,” *Microelectron. Eng.*, vol. 87, no. 10, pp. 1951–1954, Oct. 2010.

[23] Y. Guo, G. Liu, Y. Xiong, and Y. Tian, “Study of the demolding process—implications for thermal stress, adhesion and friction control,” *J. Micromechanics Microengineering*, vol. 17, no. 1, pp. 9–19, Jan. 2007.

[24] M. Koc and T. (Editor) Ozel, *Micro-Manufacturing: Design and Manufacturing of Micro-Products*. Wiley, 2011, p. 404.

[25] M. E. Dirckx, “Demolding of hot embossed polymer microstructures,” Massachusetts Institute of Technology, 2010.

[26] J. Wu and M. Gu, “Microfluidic sensing: state of the art fabrication and detection techniques.,” *J. Biomed. Opt.*, vol. 16, no. 8, p. 080901, Aug. 2011.

[27] R. K. Jena, C. Y. Yue, Y. C. Lam, P. S. Tang, and a. Gupta, “Comparison of different molds (epoxy, polymer and silicon) for microfabrication by hot embossing technique,” *Sensors Actuators B Chem.*, vol. 163, no. 1, pp. 233–241, Mar. 2012.

[28] H. Becker and U. Heim, “Hot embossing as a method for the fabrication of polymer high aspect ratio structures,” *Sensors Actuators A Phys.*, vol. 83, no. 1–3, pp. 130–135, May 2000.

[29] M. B. Esch, S. Kapur, G. Irizarry, and V. Genova, “Influence of master fabrication techniques on the characteristics of embossed microfluidic channels.,” *Lab Chip*, vol. 3, no. 2, pp. 121–7, May 2003.

[30] E. Kukharenka, M. M. Farooqui, L. Grigore, and M. Kraft, “Electroplating moulds using dry film thick negative photoresist,” *J. Micromechanics Microengineering*, vol. 13, pp. 67–74, 2003.

[31] NiCo Form, “Microfluidic Molds, Electroformed Optics, MEMS,” 2014. [Online]. Available: http://www.nicoform.com/products/microfluidics-mems-and-optics. [Accessed: 23-Sep-2014].

[32] L. J. Kricka, P. Fortina, N. J. Panaro, P. Wilding, G. Alonso-Amigo, and H. Becker, “Fabrication of plastic microchips by hot embossing.,” *Lab Chip*, vol. 2, no. 1, pp. 1–4, Feb. 2002.

[33] R. Novak, N. Ranu, and R. a Mathies, “Rapid fabrication of nickel molds for prototyping embossed plastic microfluidic devices.,” *Lab Chip*, vol. 13, no. 8, pp. 1468–71, Apr. 2013.

[34] S.-J. Kim, H. Yang, K. Kim, Y. T. Lim, and H.-B. Pyo, “Study of SU-8 to make a Ni master-mold: Adhesion, sidewall profile, and removal.,” *Electrophoresis*, vol. 27, no. 16, pp. 3284–96, Aug. 2006.

[35] C. D. Joye, J. P. Calame, M. Garven, and B. Levush, “UV-LIGA microfabrication of 220 GHz sheet beam amplifier gratings with SU-8 photoresists,” *J. Micromechanics Microengineering*, vol. 20, no. 12, p. 125016, Dec. 2010.

[36] T. Koerner, L. Brown, R. Xie, and R. D. Oleschuk, “Epoxy resins as stamps for hot embossing of microstructures and microfluidic channels,” *Sensors Actuators B Chem.*, vol. 107, no. 2, pp. 632–639, Jun. 2005.

[37] Y. Fan, T. Li, W.-M. Lau, and J. Yang, “A Rapid Hot-Embossing Prototyping Approach Using SU-8 Molds Coated With Metal and Antistick Coatings,” *J. Microelectromechanical Syst.*, vol. 21, no. 4, pp. 875–881, Aug. 2012.

[38] V. N. Goral, Y.-C. Hsieh, O. N. Petzold, R. a Faris, and P. K. Yuen, “Hot embossing of plastic microfluidic devices using poly(dimethylsiloxane) molds,” *J. Micromechanics Microengineering*, vol. 21, no. 1, p. 017002, Jan. 2011.

[39] B. Warfield, “Basic Concepts for Beginners,” *CNC Cookbook*, 2010. [Online]. Available: http://www.cnccookbook.com/CCCNCMillFeedsSpeedsBasics.htm. [Accessed: 12-Sep-2014].

[40] P. Chen, “Micromilling Manufacturing for Polymeric Biochips,” 2012, pp. 63–67.

[41] G. Rumsby, “An introduction to PCR techniques.,” *Methods Mol. Biol.*, vol. 324, pp. 75–89, Jan. 2006.

[42] C. Zhang and D. Xing, “Miniaturized PCR chips for nucleic acid amplification and analysis: latest advances and future trends.,” *Nucleic Acids Res.*, vol. 35, no. 13, pp. 4223–37, Jan. 2007.

[43] C. D. Chin, S. Y. Chin, T. Laksanasopin, and S. K. Sia, “Point-of-Care Diagnostics on a Chip,” pp. 3–22, 2013.

[44] P. Belgrader, “PCR Detection of Bacteria in Seven Minutes,” *Science (80-.).*, vol. 284, no. 5413, pp. 449–450, Apr. 1999.

[45] J. Yang, Y. Liu, C. B. Rauch, R. L. Stevens, R. H. Liu, R. Lenigk, and P. Grodzinski, “High sensitivity PCR assay in plastic micro reactors.,” *Lab Chip*, vol. 2, no. 4, pp. 179–87, Nov. 2002.

[46] O. Clerc and G. Greub, “Routine use of point-of-care tests: usefulness and application in clinical microbiology.,” *Clin. Microbiol. Infect.*, vol. 16, no. 8, pp. 1054–61, Aug. 2010.

[47] J. Wang, “Electrochemical biosensors: towards point-of-care cancer diagnostics.,” *Biosens. Bioelectron.*, vol. 21, no. 10, pp. 1887–92, Apr. 2006.

[48] W. Wu, X. Fang, J. Kong, L. Xu, X. Jiang, and H. Chen, “A portable and integrated nucleic acid amplification microfluidic chip for identifying bacteria,” *Lab Chip*, vol. 12, no. 8, p. 1495, Apr. 2012.

[49] Q. Cao, M.-C. Kim, and C. Klapperich, “Plastic microfluidic chip for continuous-flow polymerase chain reaction: simulations and experiments.,” *Biotechnol. J.*, vol. 6, no. 2, pp. 177–84, Feb. 2011.

[50] J. Kim, D. Byun, M. G. Mauk, and H. H. Bau, “A disposable, self-contained PCR chip.,” *Lab Chip*, vol. 9, no. 4, pp. 606–12, Feb. 2009.

[51] A. Bhattacharyya and C. M. Klapperich, “Thermoplastic microfluidic device for on-chip purification of nucleic acids for disposable diagnostics.,” *Anal. Chem.*, vol. 78, no. 3, pp. 788–92, Feb. 2006.

[52] A. S. Rossney, C. M. Herra, G. I. Brennan, P. M. Morgan, and B. O’Connell, “Evaluation of the Xpert methicillin-resistant Staphylococcus aureus (MRSA) assay using the GeneXpert real-time PCR platform for rapid detection of MRSA from screening specimens.,” *J. Clin. Microbiol.*, vol. 46, no. 10, pp. 3285–90, Oct. 2008.

[53] C. A. Holland and F. L. Kiechle, “Point-of-care molecular diagnostic systems--past, present and future.,” *Curr. Opin. Microbiol.*, vol. 8, no. 5, pp. 504–9, Oct. 2005.

[54] M. Worgull, J.-F. Hétu, K. K. Kabanemi, and M. Heckele, “Hot embossing of microstructures: characterization of friction during demolding,” *Microsyst. Technol.*, vol. 14, no. 6, pp. 767–773, Apr. 2008.

[55] A. Toh, Z. Wang, and Z. Wang, “Ambient hot embossing of polycarbonate, poly-methyl methacrylate and cyclic olefin copolymer for microfluidic applications,” *Des. Test, Integr. …*, pp. 1–4, 2009.

[56] J. Greener, W. Li, J. Ren, D. Voicu, V. Pakharenko, T. Tang, and E. Kumacheva, “Rapid, cost-efficient fabrication of microfluidic reactors in thermoplastic polymers by combining photolithography and hot embossing.,” *Lab Chip*, vol. 10, no. 4, pp. 522–4, Feb. 2010.

[57] L. Yi, W. Xiaodong, and Y. Fan, “Microfluidic chip made of COP (cyclo-olefin polymer) and comparion to PMMA (polymethylmethacrylate) microfluidic chip,” *J. Mater. Process. Technol.*, vol. 208, no. 1–3, pp. 63–69, Nov. 2008.

[58] H. Gong, N. Ramalingam, L. Chen, J. Che, Q. Wang, Y. Wang, X. Yang, P. H. E. Yap, and C. H. Neo, “Microfluidic handling of PCR solution and DNA amplification on a reaction chamber array biochip.,” *Biomed. Microdevices*, vol. 8, no. 2, pp. 167–76, Jun. 2006.

[59] Y.-K. Cho, J. Kim, Y. Lee, Y.-A. Kim, K. Namkoong, H. Lim, K. W. Oh, S. Kim, J. Han, C. Park, Y. E. Pak, C.-S. Ki, J. R. Choi, H.-K. Myeong, and C. Ko, “Clinical evaluation of micro-scale chip-based PCR system for rapid detection of hepatitis B virus.,” *Biosens. Bioelectron.*, vol. 21, no. 11, pp. 2161–9, May 2006.

[60] C. N. Liu, N. M. Toriello, and R. A. Mathies, “Multichannel PCR-CE microdevice for genetic analysis.,” *Anal. Chem.*, vol. 78, no. 15, pp. 5474–9, Aug. 2006.

[61] A. San-Miguel and H. Lu, “Microfluidics as a tool for C. elegans research,” *WormBook - The C. elegans Research Community*, 2013. .

[62] Harvey Tool, “Harvey Tool - Miniature End Mill,” 2014. [Online]. Available: http://www.harveytool.com/secure/Content/ImagesProducts/8a63329d-4aa5-4aa1-97fb-fa28268a136a.jpg. [Accessed: 15-Sep-2014].

[63] W.-C. Jung, Y.-M. Heo, G.-S. Yoon, K.-H. Shin, S.-H. Chang, G.-H. Kim, and M.-W. Cho, “Micro Machining of Injection Mold Inserts for Fluidic Channel of Polymeric Biochips,” *Sensors*, vol. 7, no. 8, pp. 1643–1654, Aug. 2007.

[64] Wikipedia Contributors, “Polymerase Chain Reaction,” *Wikipedia*, 2014. [Online]. Available: http://en.wikipedia.org/w/index.php?title=Polymerase_chain_reaction&oldid=623800974. [Accessed: 01-Oct-2014].

[65] S. Park, Y. Zhang, S. Lin, T.-H. Wang, and S. Yang, “Advances in microfluidic PCR for point-of-care infectious disease diagnostics.,” *Biotechnol. Adv.*, vol. 29, no. 6, pp. 830–9.

[66] A. Folch, “Liquid Smallness,” *Picasa Album*, 2000. [Online]. Available: https://picasaweb.google.com/102864211467583145284/LiquidSmallness?noredirect=1#5063034438858825346.

8. Annex

a) Arduino code for temperature control and thermocycling protocol

```
/***************************************************
  This is an example for the Adafruit Thermocouple Sensor w/MAX31855K

  Designed specifically to work with the Adafruit Thermocouple Sensor
  ----> https://www.adafruit.com/products/269

  These displays use SPI to communicate, 3 pins are required to
  interface
  Adafruit invests time and resources providing this open source code,
  please support Adafruit and open-source hardware by purchasing
  products from Adafruit!

  Written by Limor Fried/Ladyada for Adafruit Industries.
  BSD license, all text above must be included in any redistribution
 ****************************************************/

#include "Adafruit_MAX31855.h"

int thermoDO1 = 8;
int thermoCS1 = 7;
int thermoCLK1 = 6;
int thermoDO2 = 5;
int thermoCS2 = 4;
int thermoCLK2 = 3;
int tec = 9;

Adafruit_MAX31855 thermocouple1(thermoCLK1, thermoCS1, thermoDO1);
Adafruit_MAX31855 thermocouple2(thermoCLK2, thermoCS2, thermoDO2);

void setup() {
  Serial.begin(9600);
  pinMode(tec, OUTPUT);
  Serial.println("MAX31855 test");
  // wait for MAX chip to stabilize
  delay(500);
}

void holdTemp(int digTemp, int holdTime, String txtTemp){
  int start = floor(millis()/1000);
  int printTimer = floor(millis()/1000); // printTimer is a counter used to say
when to print sensor readout
  int now = floor(millis()/1000);
  int nowMin = floor(now/60);
  int nowSec = now-(nowMin*60);
  double c = thermocouple1.readCelsius();
  double c2 = thermocouple2.readCelsius();
  while(now - start <= holdTime){
    c = thermocouple1.readCelsius();
    c2 = thermocouple2.readCelsius();
    if(c<digTemp){ //temp control
      digitalWrite(tec, HIGH);}
    else if(c>digTemp){ //temp control
      digitalWrite(tec, LOW);}
    if(now >= printTimer){
      nowMin = floor(now/60);
      nowSec = now-(nowMin*60);
      Serial.print("Time: "); Serial.print("\t"); Serial.print(nowMin,DEC);
      Serial.print("m"); Serial.print(nowSec,DEC); Serial.print("s");
Serial.print("\t");
```

```
      Serial.print("Thermocouple1: "); Serial.print("\t"); Serial.print(c);
Serial.print("\t");
      Serial.print("Thermocouple2: "); Serial.print("\t"); Serial.print(c2);
Serial.print("\t");
      Serial.print(txtTemp); Serial.print("\n");
      printTimer += 2;}
    now = floor(millis()/1000);
  }
}

void holdTemp2(int digTemp, int holdTime, int heatTime, int coolTime, String
txtTemp){
  int start = floor(millis()/1000);
  int printTimer = floor(millis()/1000); // printTimer is a counter used to say
when to print sensor readout
  int now = floor(millis()/1000);
  int nowMin = floor(now/60);
  int nowSec = now-(nowMin*60);
  double c = thermocouple1.readCelsius();
  double c2 = thermocouple2.readCelsius();
  while(now - start <= holdTime){
    now = floor(millis()/1000);
    c = thermocouple1.readCelsius();
    c2 = thermocouple2.readCelsius();
    if(now >= printTimer){
      nowMin = floor(now/60);
      nowSec = now-(nowMin*60);
      Serial.print("Time: "); Serial.print("\t"); Serial.print(nowMin,DEC);
      Serial.print("m"); Serial.print(nowSec,DEC); Serial.print("s");
Serial.print("\t");
      Serial.print("Thermocouple1: "); Serial.print("\t"); Serial.print(c);
Serial.print("\t");
      Serial.print("Thermocouple2: "); Serial.print("\t"); Serial.print(c2);
Serial.print("\t");
      Serial.print(txtTemp); Serial.print("\n");
      printTimer += 2;}
    if(c<=digTemp){ // temp control
      digitalWrite(tec, HIGH);
      delay(heatTime);
      digitalWrite(tec, LOW);
      delay(coolTime);
//      Serial.print("ON"); Serial.print("\n");
    }
    else if(c>digTemp){ //temp control
      digitalWrite(tec, LOW);}
//      Serial.print("OFF"); Serial.print("\n");
  }
}

void heatTemp(int digTemp){
  // digTemp = digital sensor readout values corresponding to temperature to hold
at
//  Serial.print("Start heatTemp"); Serial.print("\n");
  digitalWrite(tec, HIGH);
  int printTimer = floor(millis()/1000);
  int now = floor(millis()/1000);
  int nowMin = floor(now/60);
  int nowSec = now-(nowMin*60);
  double c = thermocouple1.readCelsius();
  double c2 = thermocouple2.readCelsius();
  while(c < digTemp){ //temp control
    now = floor(millis()/1000);
    c = thermocouple1.readCelsius();
    c2 = thermocouple2.readCelsius();
    if(now >= printTimer){
```

```
      nowMin = floor(now/60);
      nowSec = now-(nowMin*60);
      Serial.print("Time: "); Serial.print("\t"); Serial.print(nowMin,DEC);
      Serial.print("m"); Serial.print(nowSec,DEC); Serial.print("s");
Serial.print("\t");
      Serial.print("Thermocouple1: "); Serial.print("\t"); Serial.print(c);
Serial.print("\t");
//      Serial.print("TC1 internal: "); Serial.print("\t"); Serial.print(thermoco
uple1.readInternal()); Serial.print("\n");
      Serial.print("Thermocouple2: "); Serial.print("\t"); Serial.print(c2);
Serial.print("\n");
//      Serial.print("TC2 internal: "); Serial.print("\t"); Serial.print(thermoco
uple2.readInternal()); Serial.print("\n");
      printTimer += 2;}
  }
}

void coolTemp(int digTemp){
  // digTemp = digital sensor readout values corresponding to temperature to hold
at
//  Serial.print("Start coolTemp"); Serial.print("\n");
  digitalWrite(tec, LOW);
  int printTimer = floor(millis()/1000);
  int now = floor(millis()/1000);
  int nowMin = floor(now/60);
  int nowSec = now-(nowMin*60);
  double c = thermocouple1.readCelsius();
  double c2 = thermocouple2.readCelsius();
  while(c > digTemp){ //temp control
    now = floor(millis()/1000);
    c = thermocouple1.readCelsius();
    c2 = thermocouple2.readCelsius();
    if(now >= printTimer){
      nowMin = floor(now/60);
      nowSec = now-(nowMin*60);
      Serial.print("Time: "); Serial.print("\t"); Serial.print(nowMin,DEC);
      Serial.print("m"); Serial.print(nowSec,DEC); Serial.print("s");
Serial.print("\t");
      Serial.print("Thermocouple1: "); Serial.print("\t"); Serial.print(c);
Serial.print("\t");
      Serial.print("Thermocouple2: "); Serial.print("\t"); Serial.print(c2);
Serial.print("\t"); Serial.print("\n");
      printTimer += 2;}
  }
}

void loop(){
  heatTemp(92);
  holdTemp(92, 15, "95");
  for (int x = 0; x < 107; x++ ){
    heatTemp(92);
    holdTemp(92, 10, "94");
    coolTemp(57.5);
    heatTemp(61);
    holdTemp(61, 25, "62");

  }
  heatTemp(72);
  holdTemp(72, 30, "72");
  coolTemp(30);
  Serial.print("END");
  while(1);
}
```

b) Excerpt of G-Code

```
N100 G0 G70 G90
N120 G0 G90 G54 X1.1261 Y-1.1249
N130 Z.25
N140 Z.2
N150 G1 Z-.0197 F6.42
N160 X-1.1261
N170 Y-1.0499
N180 X1.1261
N190 Y-.9749
N200 X-1.1261
N210 Y-.8999
N220 X.5601
N230 G2 X.4254 Y-.8249 I.625 J-.625
N240 G1 X-1.1261
N250 Y-.7499
N260 X.3716
N270 G2 X.347 Y-.6749 I.625 J-.625
N280 G1 X-1.1261
N290 Y-.5999
N300 X.3436
N310 G2 X.3589 Y-.5301 I.625 J-.625
N320 G1 X-.3937
N330 G2 X-.4293 Y-.525 I-.3937 J-.4051
N340 G1 X-1.1261
N350 Y-.45
N360 X-.5104
N370 G2 X-.5187 Y-.4051 I-.3937 J-.4051
N380 G1 Y-.375
N390 X-1.1261
N400 Y-.3
N410 X-.5187
N420 Y-.225
N430 X-1.1261
N440 Y-.15
N450 X-.5187
N460 Y-.075
N470 X-1.1261
N480 Y0.
N490 X-.5187
```